PALEO- AND NEOTETHYAN MARGINAL OCEANIC LITHOSPHERE REMNANTS REVEALED IN THE HIGH-GRADE BASEMENT OF THE EASTERN RHODOPE MASSIF, BULGARIA: U-PB ZIRCON AGE CONSTRAINTS AND GEODYNAMIC IMPLICATIONS

Nikolay Bonev*,✉, **Petyo Filipov**** and **Zornitsa Dotseva***

* *Department of Geology, Paleontology and Fossil Fuels, Sofia University "St. Kliment Ohridski", Bulgaria.*
** *Department of Geochemistry and Petrology, Geological Institute of the Bulgarian Academy of Sciences, Sofia, Bulgaria.*
✉ *Corresponding author: e-mail: niki@gea.uni-sofia.bg*

ABSTRACT

The eastern Rhodope Massif of Bulgaria concentrates meta-ophiolites of poorly known igneous ages, which offers the opportunity to examine the Tethyan oceanic floor and Eurasian plate margin interactions. MORB-type meta-mafic gabbro-basalt cross-cutting dykes and concordant layers to three meta-ultramafic bodies are enclosed in schist envelope. U-Pb zircon geochronology revealed crystallization ages of the dykes at 248 Ma and 245 Ma in one of the bodies, at 298 Ma for a layer at the contact of the second body and another layer at 160 Ma for the third body. Different Early Permian and Early Triassic crystallization ages of the bodies and another spatially close Late Devonian body, all witness for mantle lithosphere components that fall in the temporal range of the Paleotethys oceanic floor development and pre-Jurassic closure by subduction. As the different in age meta-ultramafic bodies are hosted by schists, this occurrence calls for a mélange related to the subduction-accretion history. This mélange telescoped during the subduction of the Paleotethys oceanic lithosphere under the Eurasian plate margin, to which accreted as early as the Middle Triassic. The mélange might well represent an element of the Paleotethys suture. The Late Jurassic crystallization age of a meta-gabbro at the contact of the third meta-ultramafic body in turn calls for the presence of Neotethys Ocean mantle lithosphere remnant, and is used to test the hypothesis for hidden mantle section of the Jurassic Evros ophiolite of the eastern Rhodope Massif. The answer is positive, and supported by the crystallization ages of the Evros ophiolite, the age of detrital zircons in the related Jurassic sedimentary successions, together with the Late Jurassic tectonic emplacement and the age of inherited Triassic-Jurassic zircons in the meta-gabbro. Thus, a Paleotethys and Neotethys oceanic floor mantle lithosphere interacted with the Eurasian plate margin and their remnants have been revealed in the eastern Rhodope Massif.

INTRODUCTION

The Rhodope Massif represents a major tectonic zone of the Alpine orogen in the northern Aegean region of the Eastern Mediterranean (Fig. 1a). In addition to the widespread occurrences of Mesozoic ophiolites in the Alpine orogen of this region (e.g., Robertson, 2002, for review), the Rhodope Massif contains also widespread occurrences of mafic-ultramafic meta-ophiolite bodies scattered within the high-grade metamorphic basement (e.g., Kozhoukharov et al., 1988). The Rhodope Massif meta-ophiolite bodies are traditionally regarded as Precambrian in age despite the lack of any sound radiometric age constraints and inferred conspicuous biostratigraphic fossil evidences (Kozhoukharova et al., 1984a; Kozhoukharov et al., 1988; Boyanov et al., 1990). Only alternatively, the meta-ophiolite bodies are largely considered as oceanic lithosphere components of the Mesozoic Tethyan oceanic floor (Burg et al., 1996; Robertson et al., 1996; Papanikolaou, 2009, 2013; Froitzheim et al., 2014). Nevertheless, the Rhodope mafic-ultramafic ophiolitic bodies offer a unique opportunity to assess the geodynamic setting and tectonic architecture at the Eurasian plate margin, and the temporal relationships of the continental margin with the Tethyan oceanic seaways.

The eastern part of the Rhodope Massif apparently concentrates the massif's mafic and mostly large ultramafic meta-ophiolite bodies (Fig. 1a), both having geochemistry that indicates MORB, MORB/IAT to IAT affinity, and thus, testifies for an ocean floor origin in spreading ridge and island arc settings (Kolcheva and Eskenazy, 1988; Mposkos et al., 1989; Bazylev et al., 1999; Haydoutov et al., 2004; Baziotis

et al., 2012; Bonev et al., 2023). The presence of Middle Ordovician comagmatic meta-gabbro and meta-plagiogranite of back-arc origin (Bonev et al., 2013a) and Late Devonian mafic protolith of a meta-eclogite (Peytcheva et al., 2018) supports the involvement of Paleozoic oceanic crust components in the build-up of the high-grade metamorphic basement. In the same area, Paleozoic mafic rock protoliths were also documented by Bauer et al. (2007), Liati et al. (2011) and Bonev (2015), with ages that straddle the Permian-Triassic boundary. However, in the eastern part of the Rhodope Massif, the magmatic crystallization age particularly for the ultramafic meta-ophiolitic bodies still remains unknown, or at least reliable age constraints for them are still unavailable nowadays. On the other side, there, the arc-related, supra-subduction zone Jurassic Evros ophiolite forms the uppermost low-grade Mesozoic unit of the eastern Rhodope metamorphic pile (see Fig. 1a). The Evros ophiolite presents only the upper crustal section of an ophiolite (Magganas, 2002; Bonev and Stampfli, 2008; 2009). Bonev and Stampfli (2008) and Bonev et al. (2010a) argued that it is more likely that part of the missing Evros ophiolite mantle section is hidden within the underlying Rhodope high-grade metamorphic basement and connected to its subduction-accretion evolution during the Alpine tectonic processes.

The incomplete magmatic age record of the aforementioned meta-ophiolites hampers to constrain more precisely the temporal range of oceanic lithosphere fragments contained in the Rhodope Massif, and particularly its eastern part, where they obviously formed in distinct past tectonic environments and different time. Therefore, any details on the age constraints of the meta-ophiolitic, especially the ultramafic
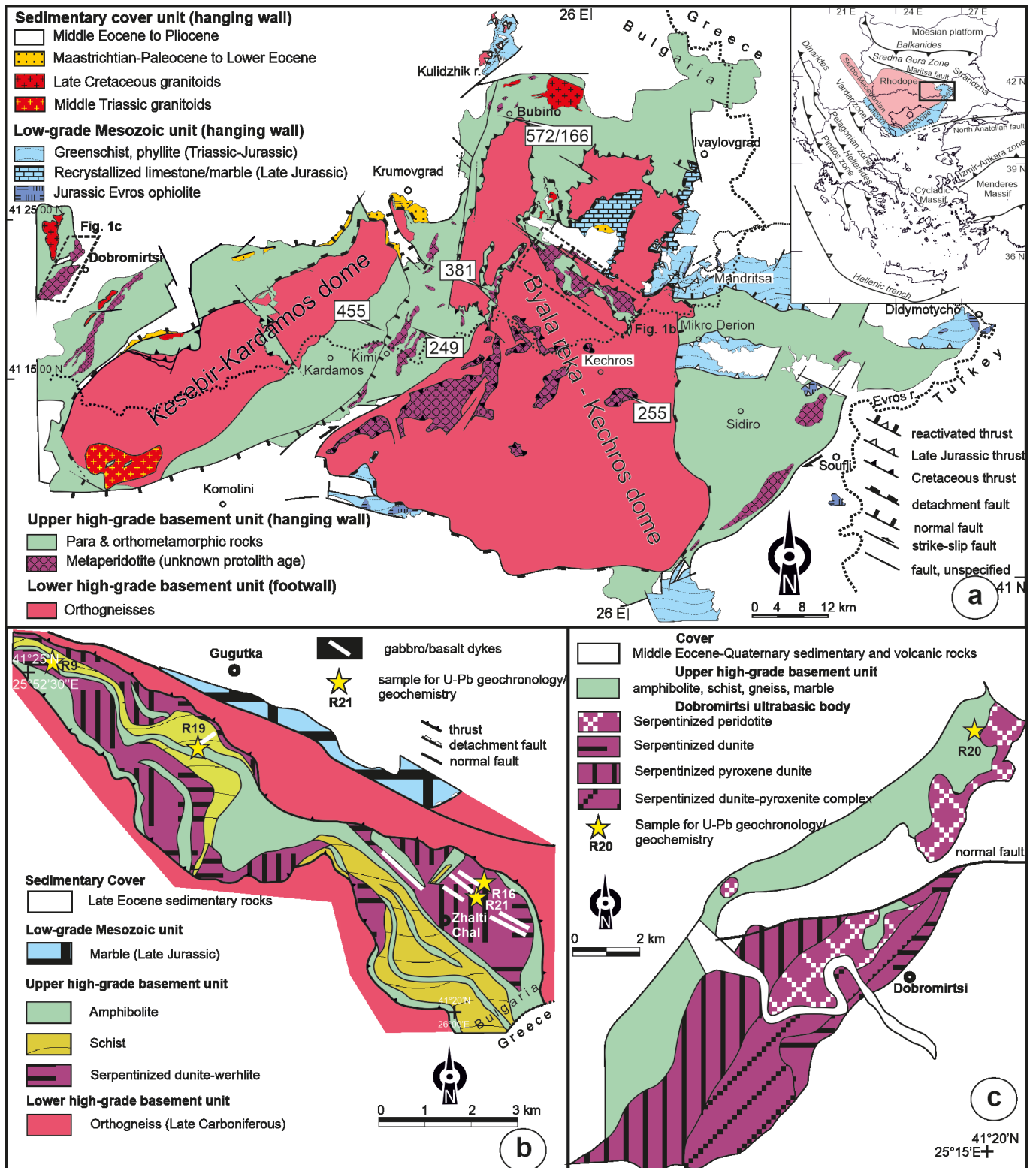
Fig. 1 - a) Synthetic geological map of the eastern Rhodope Massif in Bulgaria and Greece (modified after Bonev et al., 2015). Inset: Tectonic framework of the Alpine orogen in the northern Aegean region of the eastern Mediterranean. Boxes depict the areal extent of Fig. 1b, c. Numbers in boxes refer to available U-Pb zircon geochronology for the meta-mafic rocks. See also the text. b) Simplified geological map of the central part of the Byala reka dome (modified after Kozhoukharova, 1999). The locations of the samples studied for geochemistry and U-Pb geochronology are shown. c) Geological map of the Dobromirtsi meta-ultramafic body (modified after Nikolaev, 1958 and Payakov et al., 1963). The location of the sample studied for geochemistry and U-Pb geochronology is shown.

rocks are particularly important because they will shed new light on the span of the temporarily different oceanic lithosphere components involved in the Tethyan Ocean-Eurasian continental margin interaction during the Paleozoic and Mesozoic geodynamic evolution of this part of the Tethyan domain.

In this paper, we combine whole-rock geochemistry and U-Pb LA-ICP-MS zircon geochronology of meta-mafic rocks tightly related to the meta-ultramafic bodies in the eastern part of the Rhodope Massif. Our goal is to derive the composition and age of the meta-mafic rocks in order to establish their geo-

chemical fingerprint and temporal relations, which will allow us to distinguish distict oceanic mantle lithosphere fragments within the metamorphic pile. This will further test the hypotheses about the Tethyan oceanic seaway elements that have contributed to the crustal build-up of the crystalline basement of the Rhodope Massif, and thus the Eurasian plate margin.

GEOLOGICAL OUTLINE

General

To the north, the Rhodope Massif is separated by the Maritsa strike-slip fault zone from the Late Cretaceous volcanic arc of the Sredna Gora Zone, and to the south, the southern parts of the Rhodope Massif are hidden in the Aegean Sea (Fig. 1a, inset). To the east, the Rhodope Massif is overlain by the sedimentary deposits of the large Cenozoic Thrace basin exposed in Greece, Bulgaria and Turkey, and to the west, it underlies the Serbo-Macedonian Massif (Fig. 1a, inset). The Rhodope Massif (together with the Serbo-Macedonian Massif) is regarded as a crustal-scale thrust complex assembled by southward thrusting in the hanging wall of a north-dipping Late Cretaceous-Cenozoic subduction zone located in the Vardar Zone (Burg et al., 1996; Ricou et al., 1998; Burg, 2012). In this convergent setting, the Rhodope nappe stacking associated with amphibolite-facies metamorphism resulted in crustal thickening, which was accompanied by a coeval and subsequent extension (Koukouvelas and Doutsos, 1990; Dinter and Royden, 1993; Burg et al., 1996; Dinter, 1998; Bonev et al., 2006; Bonev and Beccaletto, 2007; Brun and Sokoutis, 2018). Generally, the Rhodope Massif is dominated by amphibolite-facies metamorphic basement consisting of pre-Alpine and Alpine (e.g., Lips et al., 2000; Liati, 2005; Liati et al., 2011) units of continental and oceanic origin that are intruded by voluminous Late Cretaceous to Miocene granitoids (Meyer, 1968; Soldatos and Christofides, 1986; Zagorchev et al., 1987; Dinter et al., 1995; Christofides et al., 2001; von Quadt and Peytcheva, 2005; Marchev et al., 2013). Maastrichtian-Paleocene to Pliocene-Quaternary sedimentary rocks (Ivanov and Kopp, 1969; Zagorchev, 1998; Boyanov and Goranov, 2001 and references therein) and Oligocene volcanic and volcanic-sedimentary sequences (Innocenti et al., 1984; Del Moro et al., 1988; Harkovska et al., 1989; Christofides et al., 2004; Marchev et al., 2010) represents cover sequences.

Geological setting of the eastern Rhodope Massif

The regional-scale tectonic architecture of the eastern Rhodope Massif is represented by late Alpine extensional core complex-type metamorphic domes, namely the Kesebir-Kardamos and the Byala reka-Kechros domes (Fig. 1a, Bonev, 2006; Bonev et al., 2006). These structures expose four principal units, mainly bounded by extensional tectonic contacts of Early Eocene low-angle detachments. The distinct units are subdivided according to their structural setting in the footwall and hanging wall of the extensional system, and the tectono-metamorphic history and radiometric ages of consistent lithologies. From the base to the top, these units are (Bonev, 2006): (i) a lower high-grade basement unit, (ii) an upper high-grade basement unit, (iii) an overlying low-grade Mesozoic unit, and (iv) a sedimentary and volcanic unit of Cenozoic cover sequences (Fig. 1a). In addition, Late Cretaceous to Oligocene-aged granitoids intruded the high-grade basement units (Del Moro et al., 1988; Pe-Piper and Piper, 2002; Ovtcharova et al., 2003; Marchev et al., 2006).

In the footwall of the extensional system, the lower high-grade basement unit mainly consists of orthogneisses and migmatites intercalated with minor paragneiss and amphibolite layers, and thus this unit unequivocally shows a clear continental affinity. Late Carboniferous to Late Permian granitoid protolith U-Pb zircon ages in the range of 326-254 Ma were reported for the orthogneisses (Peytcheva and von Quadt, 1995; Cornelius, 2008; Liati et al., 2011), which indicates that Late Paleozoic acid crustal fragments were subsequently involved in the nappe and extensional systems during the Mesozoic deformation and metamorphism.

The upper high-grade basement unit is a heterogeneous metamorphic succession of continental and oceanic affinity lithologies consisting of intercalated meta-sedimentary and meta-igneous rocks. This is the basement unit that comprises widespread occurrences of mafic and ultramafic meta-ophiolite bodies that are focus of this study.

In the upper high-grade basement unit, the ultramafic rocks are represented by numerous bodies and lenses that range in size from several kilometres to a meter scale. The ultramafic rocks consist of three series, namely refractory mantle harzburgite and cumulate dunite-orthopyroxenite series with MORB affinity, and cumulate dunite-wehrlite-clinopyroxenite series of supra-subduction zone-like geochemical signature (Bazylev et al., 1999 and references therein; Kolcheva et al., 2000). The ultramafic rocks, together with the low-K mafic volcanic and plutonic rocks thwiin the unit, are considered as metamorphosed fragments of dismembered Precambrian ophiolite association (Kozhoukharova 1984a). Kozhoukharova (1984a) chemically distinguishes high-Ti, high-Al and high-Fe subgroups within the volcanic and plutonic members of the meta-ophiolite association, among which the most common rock types are meta-gabbro-norite, meta-gabbro, meta-gabbro-diorite, all transformed into amphibolite that preserves relics of primary magmatic minerals and textures. Although these amphibolites resulted from the main amphibolite-facies metamorphism, they also preserve relic high-pressure (eclogite) assemblages (i.e. eclogite-amphibolite, Mposkos and Perdikatsis, 1989; Baziotis et al., 2008; 2014), and display MORB-like geochemistry of oceanic crust tholeiite basalt protolith (Kolcheva and Eskenazy, 1988). A geochemical study of the amphibolites in northern Greece has shown their magmatic origin, whose protoliths were tholeiites with oceanic floor MORB/IAT affinities, the latter affinity more pronounced in the amphibolites from the eastern Rhodope Massif (Mposkos et al., 1989). Haydoutov et al. (2004) have documented the island-arc origin of amphibolites with an arc tholeiitic to boninitic affinity. Recently, Bonev et al. (2023) have documented MORB to supra-subduction zone signatures of high- and low Ti groups of amphibolites i.e. the mafic ophiolitic rocks within the upper high-grade basement unit, both in Bulgaria and Greece.

U-Pb zircon crystallization ages of magmatic protoliths are only available for the amphibolites in the upper high-grade basement unit. Carrigan et al. (2003) have reported an age of 572±5 Ma for a meta-gabbro, however, recent dating revealed a Middle Jurassic crystallization age (166.8±0.96 Ma, Filipov et al., 2022). An age of 380.9±1.9 Ma (Peytcheva et al., 2018) was reported in amphibolitized eclogite at the rim of a peridotite body, whereas a range of ages from 287±5.5 Ma to 199±1.8 Ma in the cores of zircons from other eclogite lens have been reported by Bauer et al. (2007). Liati et al. (2011) have reported ages of 255.8±2.1 Ma and ~ 250 Ma for gabbroic protolith of eclogites. Several zircons in amphibolite rimming a peridotite yielded magmatic core ages at 850

Ma, 573 Ma, 502 Ma, 389 Ma and 249 Ma (Bonev, 2015). MORB-IAT affinity meta-gabbro, meta-plagiogranite and garnet-amphibolite, which are interpreted to have protoliths formed in a back-arc rift-spreading setting, yielded a mean age of 455 Ma for the magmatic crystallization (Bonev et al. 2013a). Noteworthy, the ages of orthogneisses with granitoid protolith dated at 160 Ma and 154 Ma, which cross-cut an amphibolite and amphibolitized eclogite (Bonev et al., 2015), respectively, imply at least Late Jurassic minimum crystallization age of the amphibolite/eclogite protoliths. Actually, the radiometric ages for Jurassic acid magmatic bodies appear more abundant in the upper high-grade basement unit (e.g., Cornelius, 2008; Liati et al., 2011; Bonev et al., 2015), while the mafic bodies of the same age are much less frequent and/or even single.

The main amphibolite-facies and relict eclogite-facies metamorphism in the eastern Rhodope high-grade basement units (Liati and Mposkos 1990; Mposkos and Liati, 1993) locally reached ultrahigh-pressure conditions (Mposkos and Kostopoulos, 2001), and therefore indicate a complex Alpine tectono-metamorphic history bracketed between 158 Ma and 42 Ma (Liati, 2005; Liati et al., 2011). Both high-grade basement units in Paleocene to Late Eocene (63-34 Ma) times gradually cooled below 300-500°C from the hanging wall to the footwall of the extensional system as derived from $^{40}Ar/^{39}Ar$ ages (e.g., Bonev et al., 2013b).

The low-grade Mesozoic sequences (Papadopoulos et al., 1989; Boyanov et al., 1990) form a separate unit, which is regarded as the eastern extension of the Circum-Rhodope Belt defined in the Chalkidiki Peninsula of northern Greece (e.g., Kauffmann et al., 1976; Papanikolaou, 2009). The low-grade Mesozoic unit, forming part of the hanging wall, consists of Triassic-Late Jurassic metasandstones, marbles, greenschists and phyllites (Bonev and Stampfli, 2008; Meinhold and Kostopoulos, 2013) and Early-Middle Jurassic island arc tholeiitic basalt-andesite lava flows, meta-pyroclastic rocks and intrusive rocks of the Evros ophiolite (Bonev et al., 2015 and references therein). Stratigraphically, they are overlain by Early Cretaceous limestones (Ivanova et al., 2015), which seal the Late Jurassic low-grade metamorphic and tectonic emplacement history (ca. 157-154 Ma, Bonev et al., 2010b; Bonev and Stampfli, 2011). Based on the petrology and geochemistry of the arc magmatic suite and the bulk lithologic context, the low-grade Mesozoic unit is interpreted as a Jurassic-Early Cretaceous island arc-accretionary assemblage, originally located along the northern active margin of the Vardar Ocean (Bonev and Stampfli, 2003; 2008; Bonev et al., 2015).

The sedimentary and volcanic unit includes Maastrichtian-Paleocene to Pliocene sequences (Boyanov and Goranov, 2001). The Maastrichtian-Paleocene to Middle Eocene syn-tectonic hanging wall sedimentary rocks which fill supra-detachment half-grabens, and also occurring in fault contact with the detachment (Bonev et al., 2006), are limited by graben-bounding faults or lying unconformably over the high-grade basement units. The Maastrichtian-Paleocene sedimentary rocks are unconformably overlain by Middle Eocene sedimentary rocks, which are in turn unconformably overlain by Late Eocene-Oligocene sedimentary rocks. The latter sedimentary rocks are accompanied by Late Eocene-Oligocene volcanic and sedimentary-volcanogenic sequences (Harkovska et al., 1989). The topmost Miocene-Pliocene sedimentary rocks represent a new transgressive cycle covering unconformably the metamorphic basement units and the Paleogene successions.

FIELD DATA, SAMPLES AND PETROGRAPHY

Our study focuses on three meta-ultramafic bodies in the eastern Rhodope Massif, namely Zhalti Chal body, Kazak body and Dobromirtsi body, named after their location at the vicinity of the eponymous villages. Zhalti Chal body is one of several meta-ultramafic bodies exposed in the central part of the Byala reka-Kechros dome, together with the Kazak body (Fig. 1a, b), whereas the Dobromitsi meta-ultramafic body occurs at the western tip of the eastern Rhodope Massif (Fig. 1a, c). In the central Byala reka dome, the meta-ultramafic bodies being part of the upper high-grade basement unit are included in a thrust sheet emplaced onto the lower high-grade basement unit (Fig. 1b, see also Bonev, 2006).

Zhalti Chal meta-ultramafic body is rimmed by amphibolites, and both lithologies are hosted by two-mica schists in the southwest and schists and gneisses to the northeast (Fig. 1b). It is elongated NW-SE and parallels the regional foliation of the host lithologies. The Zhalti Chal meta-ultramafic body consists of serpentinized dunites and wehrlites (Bazylev et al., 1999), in which Kozhoukharova (1999) has reported occurrences of several dyke-like bodies of metasomatic gabbros, and the dykes were also confirmed by Haydoutov et al., (2004). The former author considers the metasomatic gabbros of metamorphic origin. Our field observations confirmed the existence of mafic, meta-gabbroic dykes cross-cutting the Zhalti Chal meta-ultramafic body. These dykes up to several meters-thick strike ESE (100-120°), have subvertical attitude or very steeply dip to the southwest. The dykes are metamorphosed into massive amphibolites. These massive amphibolites are medium- to coarse-grained homogeneous meso-melanocratic rocks with granoblastic and foliated textures, showing occasionally well-developed mineral lineation delineated by the plagioclase. In thin sections, the amphibolite mainly consists of amphibole and plagioclase, and epidote-zoisite, ± Fe-Ti oxides and rare quartz complements the mineral assemblage as the minor mineral phases (Fig. 2 a, b). According to Kozhoukharova (1999), the plagioclase has composition mainly of oligoclase-andesine, while the amphibole is actinolite-magnesium-hornblende. Accessory minerals are rutile, titanite, zircon and rare apatite. Epidote-zoisite group minerals are products related to the metamorphic processes and developed both around the amphibole and plagioclase crystals. Two samples R16 and R21 from two separate dykes were selected for geochemistry and geochronology (Fig. 1b for location, see also Fig. 2a, b).

The Kazak meta-ultramafic body is also elongated NW-SE, rimmed by amphibolites, and hosted by two-mica schists. This body consists of fine-grained lherzolite composed of olivine, clinopyroxene and amphibole (Bazylev et al., 1999). To the north, it is overlain by a thin layer of massive garnet-bearing amphibolites, likely amphibolitized eclogites, as previously documented by Kozoukharova (1984b) at the village of Kazak. Sample R9 was collected from the garnet-bearing amphibolite, for which mineral and chemical compositions were already presented (Bonev et al., 2023). The sample R9 demonstrates chemical composition consistent with a high Ti gabbroic-basaltic protolith.

Kozhoukharova (1999) has also reported small basalt dykes intruding the schists to the north of the Kazak meta-ultramafic body (see Fig. 1b). According to the latter author the dykes are high-Ti tholeiites turned into garnet amphibolites by subsequent metamorphic processes. Sample R19 was collected from a single meta-basalt dyke, which represents fine-grained garnet-bearing amphibolite that strikes NNE (30°)
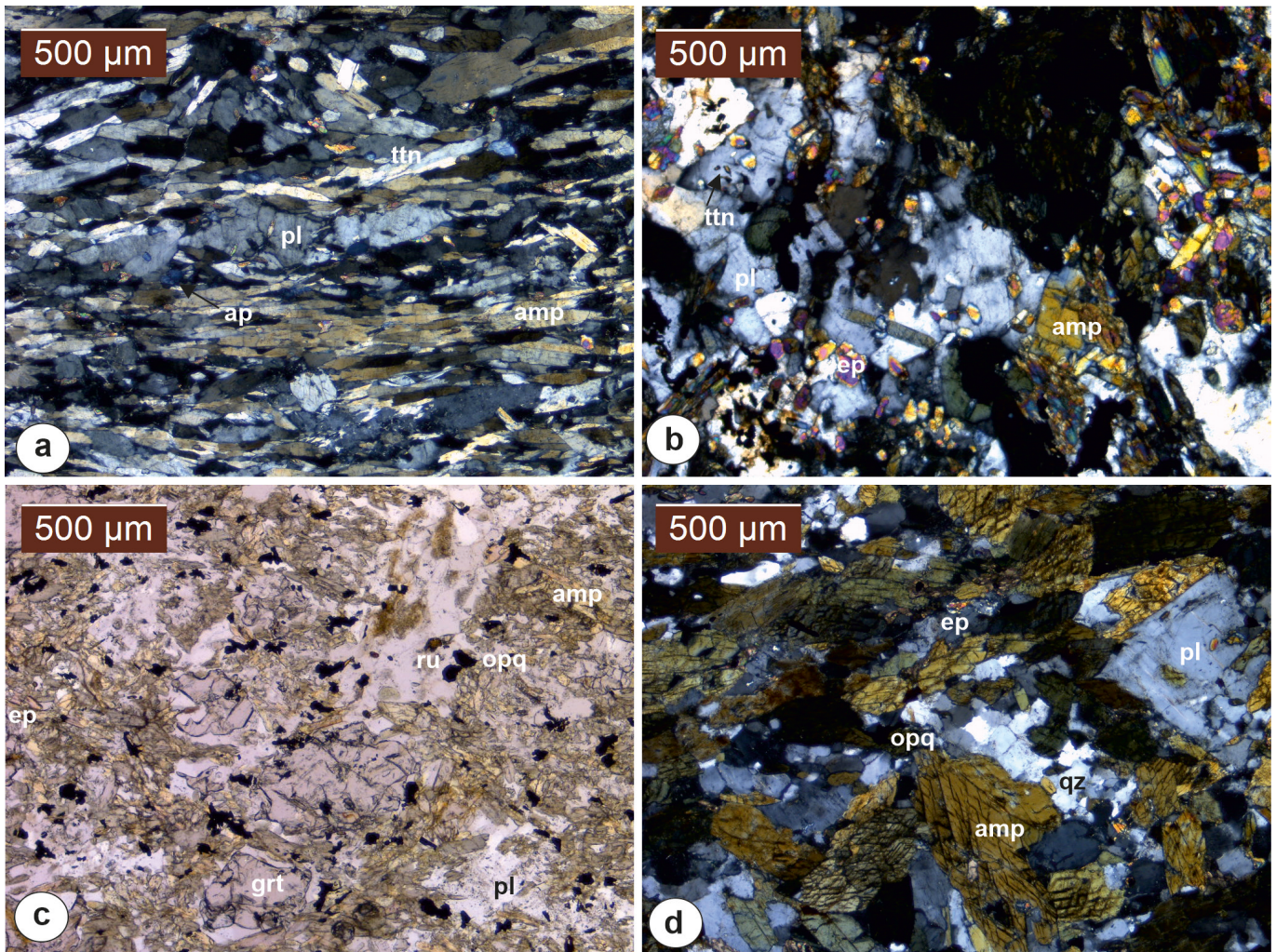
Fig. 2 - Photographs of the studied meta-mafic rocks. a) microphotograph of sample R16, b) microphotograph of sample R21, c) microphotograph of garnet amphibolite sample R19, d) microphotograph of meta-gabbro sample R20. Microphotographs in crossed polarisers are in a, b and d, and c is in plane polarised light. Mineral abbreviations (after Whitney and Evans, 2010): amp, amphibole; ap, apatite; grt, garnet; ep, epidote; opq, opaque; pl, plagioclase; ru, rutile; ttn, titanite; qz, quartz.

and lays oblique to the regional foliation in the host schists. In sample R19 amphibole and plagioclase are the main mineral constituents, together with disseminated Fe-Ti oxides (Fig. 2c). Garnet and epidote-zoisite group minerals of metamorphic origin complement the mineral assemblage. Accessory minerals include apatite and titanite. As the Fe-Ti oxides are included in plagioclase and amphibole, this account for the presence of a primary magmatic opaque mineral phase (Fig. 2c). Sample R19 was used only for geochemistry.

At the Central-Eastern Rhodope boundary the Dobromirtsi meta-ultramafic body is elongated NE-SW, a large part of this body is covered by Eocene-Oligocene sedimentary rocks, and only to the west it is overlain by other lithologies of the upper high-grade basement unit (Fig. 1c). The Dobromirtsi body consists of dunite-harzburgite and dunite-clinopyroxenite/orthopyroxenite, which exhibits dunite-harzburgite-clinopyroxenite layering in its western part (Bazylev et al., 1999). Our field observations in the northern part of Dobromirtsi body revealed that this body has direct magmatic contact with mafic rocks transformed into massive amphibolites. These massive amphibolites are medium- to coarse-grained, consisting of amphibole and plagioclase as major mineral phases, and subordinate Fe-Ti oxides. Plagioclase is rarely lamellar, but visibly has preserved the original igneous grain

sizes (Fig. 2d). The occurrence at the contact with the meta-ultramafic body and textural features of the amphibolites most likely indicate its original gabbroic protolith. Accessory minerals in amphibolites include apatite, zircon and titanite. Epidote-group minerals are metamorphic in origin, and developed mainly at the rims of the plagioclase crystals. Sample R20 was sampled from the aforementioned amphibolite for geochemistry and geochronology.

METHODS

Whole-rock samples were crushed using a steel jaw crusher and a hydraulic press to finally be powdered to < 70 µm using a mortar agate mill at the Sofia University "St. Kliment Ohridski". Major elements were analyzed on fused glass beads of mixed approximately 1 g of powdered sample with 3 g of lithium metaborate ($LiBO_2$) and 6 g of lithium tetraborate ($Li_2B_4O_7$) flux. The melting process was realized using a Claisse LeNeo Fused Bead maker, in 5% Au-95% Pt casting bowls at 1065°C. The loss of ignition (LOI) at 1000°C was expressed as a percentage of sample weight dried in an oven at 110°C overnight. An X-ray fluorescence (XRF) PANalytical (EDXRF, Epsilon 3XLE, Omnian 3SW) instrument at the

University of Sofia "St. Kliment Ohridski", Bulgaria was used for the analyses. Analytical errors for major oxides are within the range of 1%. The trace element and REE were analyzed by LA-ICP-MS on the same glass beads used for XRF analyses on a New Wave UP193FX LA coupled to a Perkin Elmer ELAN DRC-e quadrupole ICP-MS at the Geological Institute of the Bulgarian Academy of Sciences. Analytical procedures are the same as described in Bonev et al. (2019a). Analytical results are listed in Table 1, together with sample locations.

Zircon for U-Pb dating was recovered from jaw crushed and milled rock samples using a Wilfley shaker table, followed by magnetic and heavy liquid ($CHBr_3$ and CH_2I_2) separation at the Geological Institute of the Bulgarian Academy of Sciences. Zircon grains were hand-picked under a binocular microscope and thermally annealed at 900°C for 48 h in a muffle and afterwards mounted in epoxy resin and polished.

Table 1- Whole-rock chemical composition of the meta-mafic rocks from the eastern Rhodope Massif.

Sample	R16	R19	R20	R21
Rock type	amp	grt amp	amp	amp
Location	Zhalti Chal	Gugutka	Dobromirtsi	Zhalti Chal
	N41°22'36''E26°0'16''		N41°26'42''E26°16'34''	N41°22'8.2''E25°59'59.9''
SiO_2	47.62	47.37	52.08	43.37
TiO_2	1.36	2.34	1.76	2.24
Al_2O_3	16.53	16.04	15.22	17.95
Fe_2O_3	10.63	12.52	11.88	14.16
MnO	0.18	0.23	0.18	0.16
MgO	6.59	7.81	5.3	6.81
CaO	12.7	7.95	6.91	10.85
Na_2O	2.37	3.65	4.54	2.35
K_2O	0.37	0.16	0.35	0.16
P_2O_5	0.09	0.2	0.11	0.12
SO_3	-	0.12	-	-
LOI	1.52	1.56	1.64	1.81
Total	99.96	99.95	99.97	99.98
Nb	4	6	4	2
Zr	102	185	129	27
Y	31	38	41	25
Rb	6	4	24	2
Sr	275	239	155	217
Cs	-	-	1	-
Ba	91	61	34	53
Th	1	1	1	0.2
U	1	0.3	0.4	0.1
Pb	10	12	21	4
Ta	0.5	0.5	0.2	0.1
Hf	4	4	4	-
Sc	36	35	36	64
Cr	273	237	140	90
V	263	316	340	705
Ni	51	75	25	38
Ga	14	16	16	19
Zn	83	118	55	48
Cu	167	75	203	52
Co	35	36	32	39
La	7	11	6	3
Ce	16	27	17	8
Pr	2	4	3	1
Nd	12	20	14	8
Sm	4	6	5	3
Eu	1	2	2	1
Gd	5	6	6	4
Tb	1	1	1	1
Dy	5	7	7	5
Ho	1	1	1	1
Er	3	4	5	3
Tm	0.5	1	1	0.4
Yb	3	4	4	3
Lu	0.5	0.5	1	0.4

abbreviations: amp, amphibolite; grt amp, garnet amphibolite

Optical cathodoluminescence (CL) imaging was carried out for identifying inherited cores, cracks and inclusions inside the crystals using a motorized optical system Cathodyne New-Tec Scientific attached to microscope Leica 2700 at the Geological Institute of the Bulgarian Academy of Sciences and JEOL JSM-6610 LV SEM-EDS at the University of Belgrade, Serbia. U-Pb in-situ zircon dating was performed at the LA-ICP-MS laboratory of the Geological Institute using a New Wave UP193FX LA coupled to a Perkin Elmer ELAN DRC-e quadrupole ICP-MS. Ablation parameter was set up to diameter of 35 μm, frequency of 8 Hz and detection time within 0.002-0.003 s. Analyses were calibrated with the GEMOC-GJ1 zircon (Jackson et al., 2004) as an external standard for fractionation correction. Plešovice (Slama et al., 2008) and 91500 (Wiedenbeck et al., 1995) zircons were used as unknowns, and used to correct the systematic errors. Data reduction was processed using Iolite v. 2.5 (Paton et al., 2011), applying down-hole fractionation correction. Diagram plots and concordia ages were obtained using Isoplot 4.15 (Ludwig, 2011). Kernel Density Estimate was assessed using the online application IsoplotR (Vermeesch, 2018). Analytical data of U-Pb zircon geochronology of the samples are presented in Supplementary Table 1S. Twenty-five to forty-five zircon crystals were analyzed for each distinct mafic rock sample.

WHOLE-ROCK GEOCHEMISTRY

The studied mafic rocks turned into amphibolites cover the range of basic compositions with SiO_2 (47.37-52.08 wt.%) (Table 1). They are characterized by a high content of TiO_2 (1.36-2.34 wt.%). The MgO content ranges from 5.30 to 7.81 wt.%. CaO content is moderate 5.91-12.70 wt.%, and Al_2O_3 ranges from 15.31 to 17.95 wt.%. Alkali contents are variable, generally elevated (av. total alkali > 3.49 wt.%), with a high Na/K ratio (Table 1).

In terms of the trace elements, the studied amphibolites show the following features (Table 1): (i) high abundances of some incompatible elements (e.g. Nb, Y, Zr), (ii) identical Hf, similar Ta and Sc concentrations; (iii) relatively low Cr (90-273 ppm), elevated V (263-705 ppm) and low Ni (< 200 ppm) contents. The low Ni and Cr contents in the amphibolites do not meet the criteria for primitive mantle-derived melts for their precursors. Therefore, the major and trace element abundances of the amphibolites classify them as low-K and high-Ti igneous protoliths of gabbroic (basaltic) composition, as also deduced from their petrographic features.

The amphibolites display REE abundances higher than the chondrite, showing flat patterns on the chondrite-normalized diagram that characterize the ocean floor basalts (Fig. 3a).
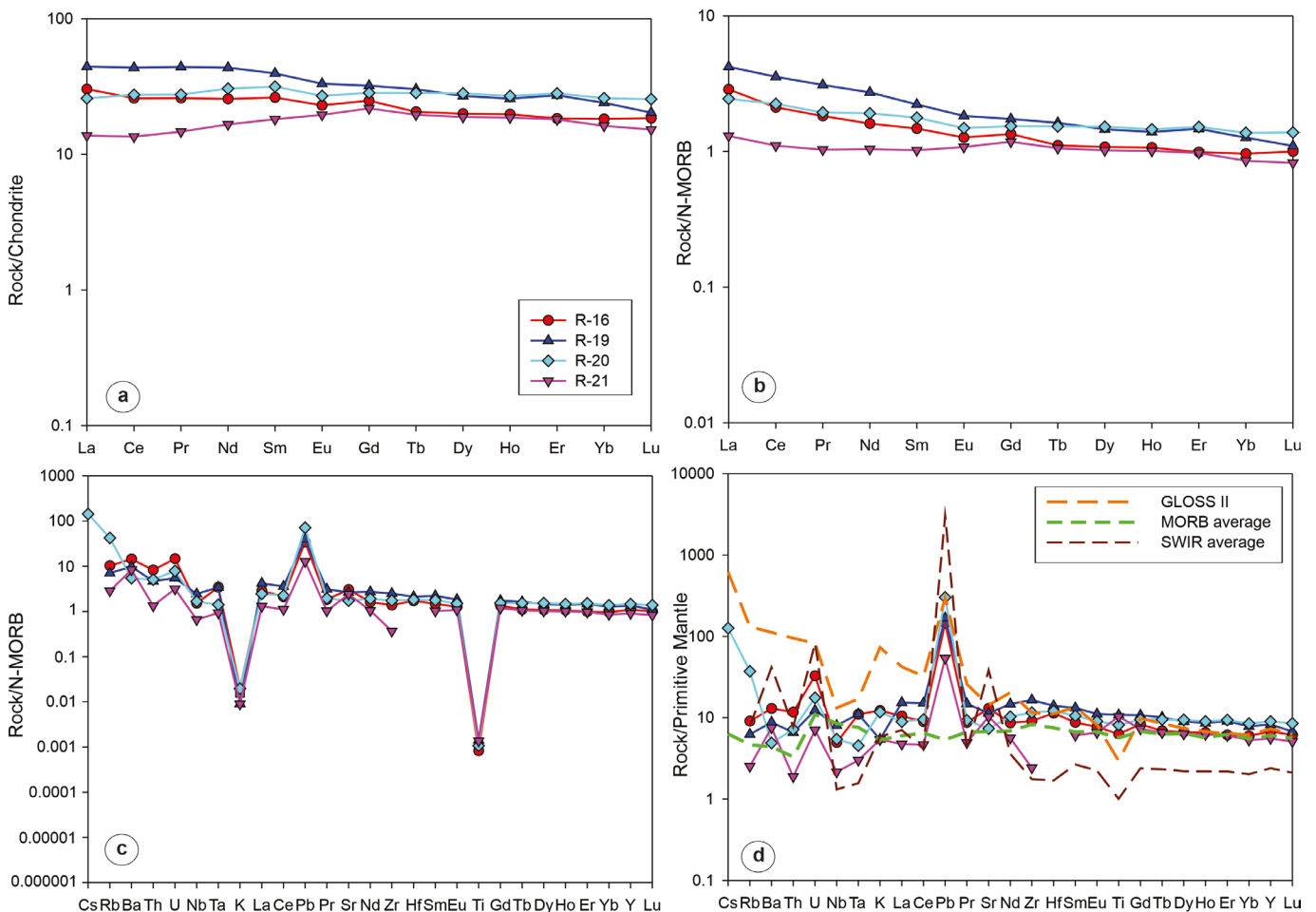

Fig. 3 - REE and trace elements diagrams for the studied meta-mafic rocks: a) chondrite-normalized (McDonough and Sun, 1995) REE patterns, b) N-MORB-normalized (Sun and McDonough, 1989) REE diagram, c) N-MORB-normalized (Sun and McDonough, 1989) multi-element diagram, d) primitive mantle normalized (Sun and McDonough, 1989) multi-element diagram for the studied meta-mafic rocks and average compositions of mid-ocean ridge basalts (MORB) from Kelemen et al. (2014), volcanic and biogenic sediments from Southwest Indian Ridge (SWIR) after Chen et al. (2021) and globally subducting sediment (GLOSS II) composite (Plank, 2014).

The normal mid-ocean ridge basalt (N-MORB) normalized patterns are subparallel, lying close to this mantle composition, and demonstrate a slight LREE enrichment (Fig. 3b). N-MORB normalized multi-element diagram demonstrates high ratios of large-ion lithophile elements (LILE) relative to high-field strength elements (HFSE) (Fig. 3c). However, the amphibolites show flat HFSE and REE patterns that overlap N-MORB composition. A positive Pb anomaly and negative K and Ti anomalies characterizes the studied rocks. These anomalies on N-MORB normalized diagram suggest a weak subduction-related and/or crustal input in the magma source. This is indicated by profiles on primitive mantle normalized multi-element diagram (Fig. 3d), in which the studied rocks deviate from this averaged mantle composition, overlap MORB composition and show chemical similarity to GLOSS II and partial similarity to SWIR, which support the subduction-related influence.

Overall, the N-MORB overlapping abundances of the HFSE and REE in the amphibolites suggest a magma source that is very close to the typical N-MORB, with a weak subduction zone influence.

U-PB ZIRCON GEOCHRONOLOGY

Because of the intrusive relationships of the former gabbro dykes with the Zhalti Chal meta-ultramafic body, as well as the gabbroic rocks occurrences in direct magmatic contact with the Kazak and Dobromirtsi meta-ultramafic bodies, these mafic lithologies are extremely useful to provide insights into the igneous age of these meta-ultramafic bodies. To constrain the timing of the mantle lithosphere resulting from ocean floor magmatism in the eastern Rhodope Massif, we have dated above described four meta-mafic samples by U-Pb zircon geochronology.

The Zhalti Chal meta-gabbro dyke (sample R16) hosts euhedral mainly prismatic zircons with a length of up to 200 μm. In the CL images they display magmatic oscillatory and sector zoning patterns (Fig. 4a, b). Four concordant analyses out of twenty-seven crystals analyzed from sample R16 yielded a concordant age of magmatic crystallization at 247.8±2.3 Ma (Fig. 5a). In addition, several concordant clusters point to inheritance revealed by three zircons at 605.6±6.6 Ma, two zircons at 551.3±16 Ma, and other two zircons at 478.1±3.1 Ma, four crystals at 328.9±3.9 Ma, two grains at 305.8±2.2 Ma, and several single zircons gave concordant ages at 2095±16 Ma, 784±14 Ma, 663.4±8.4 Ma, 458.0±5.9 Ma, 378.6±4.8 Ma, 359.0±4.1 Ma and 278.1±3.6 Ma (see Supplementary Fig. 1S). Kernel density estimate (KDE) diagram displays a prominent peak of age distribution at around 250 Ma (Fig. 6a). The four youngest age-constraining concordant zircons are characterized by high Th/U ratios of 0.17 to 1.23, which are typical for magmatic zircons (Rubatto, 2002; Tiepel et al., 2004) (see Supplementary Table 1S).

The Zhalti Chal meta-gabbroic dyke (sample R21) comprises mostly zircons with a homogeneous pattern, which exhibit mainly pyramidal and prismatic and rarely ovoid shapes that vary in size from 80 to 200 μm in CL images (Fig. 4c, d). Two zircon analyzes yielded a concordia age of 244.7±3.1 Ma (Fig. 5b), which is interpreted as the magmatic crystallization age of the gabbroic protolith. These two concordant zircons are characterized by high Th/U ratios of 0.77 and 1.57. In addition, two xenocrystic zircons delivered concordia at 381.6±1.7 Ma and other two xenocrystic zircons gave an age at 324.3±2.3 Ma, three zircons are concordant

at 296.5±3.3 Ma, and two zircons yielded a concordia age at 271.8±2.8 Ma. Several single zircons gave concordant ages at 418.4±4.5 Ma, 402.9±3.1 Ma, 393.6±3.3 Ma, 381.6±7.1 Ma, 355.7±5.0 Ma, 324.3±2.3 Ma and 281.5±2.9 Ma (see Supplementary Table 1S and Fig. 1S). In the KDE diagram is visible a peak at around 250 Ma (Fig. 6b). Two groups of discordant analyses deliver lower intercepts at 137±74 Ma and 97±5 Ma reflecting probably the timing of metamorphic events (Fig. 6b).

Zircons from the Kazak garnet amphibolite (sample R9) exhibit well-preserved magmatic oscillatory and sector zoning patterns in euhedral crystals of prismatic and pyramidal shapes (Fig. 4e, f). Three concordant zircons out of twenty-five crystals analyzed from sample R9 yielded a magmatic crystallization age of 297.6±4.6 Ma (Fig. 5c). Several groups of two zircons each yielded concordia ages at 510.3±3.6 Ma, 497.1±4.2 Ma, 428.1±4.1 Ma and 405.5±4.5 Ma. Three zircons defined a concordia age at 313.3±1.9 Ma, and single zircons are concordant at 479.5±4.8 Ma and 464.4±6.0 Ma (see Supplementary Fig. 1S). Magmatic age-defining concordant zircons have Th/U ratios in the range of 0.40-0.52. Inherited zircons have Th/U ratios in the range 0.18-0.96 (see Supplementary Table 1S). The KDE diagram illustrates a youngest peak of probability density at about 300 Ma (Fig. 6c).

Sample R20 from the Dobromirtsi amphibolites contains mostly magmatic oscillatory- and rarely sector-zoned euhedral zircons, which exhibit prismatic shapes and vary in size from 100 to 250 μm (Fig. 4g, h). Unzoned recrystallized rims are frequently observed to embrace zonal cores. Four zircons out of forty-five crystals analyzed yielded the youngest concordia age of 160.1±1.8 Ma (Fig. 5d). Six inherited zircons gave a concordia age of 214.9±2.4 Ma, five zircons yielded a concordia age of 232.7±2.4 Ma, four defined a concordia age at 250.9±3.5 Ma, three gave concordia age at 196.3±4.3 Ma, and several zircon pairs are concordant at 502±39, Ma, 239.8±2.0 Ma, 220.9±8.6 Ma and 182.5±1.9 Ma (see Supplementary Fig. 1S). A single inherited zircon yielded a concordant age at 281.7±3.9 Ma. The Kernel probability density points to a peak at around 220 Ma (Fig. 6d), which is highly unlikely considering the high mean squared weighted deviation (MSWD) varying 5.1 to 6.9 for concordant clusters at 214.9±2.4 and 220.9±8.6 respectively (see Supplementary Fig. 1S). The most probable age for the protolith crystallization is within 196-160 Ma characterized by lower MSWD 1.3-2.5 and higher probability of concordance 0.12-0.25 (see Fig. 6d and Supplementary Fig. 1S). We consider the youngest concordant cluster of 160.1±1.8 Ma to reflect the crystallization age of the Dobromirtsi gabbroic protolith. In sample R20 crystallization age-defining concordant zircons are characterized by high Th/U ratios of 0.12-0.47 (see Supplementary Table 1S).

DISCUSSION

Composition and ages

Our petrographic results give evidence that the studied meta-mafic rock associated with meta-ultramafic bodies in the upper high-grade basement unit of the eastern part of the Rhodope Massif have magmatic textures of their protoliths significantly obliterated by recrystallization during the metamorphic processes and deformation. The original igneous grain shape and size are only occasionally preserved. These own observations confirm previous research on metamorphic petrology of the mafic rocks in the crystalline basement of the
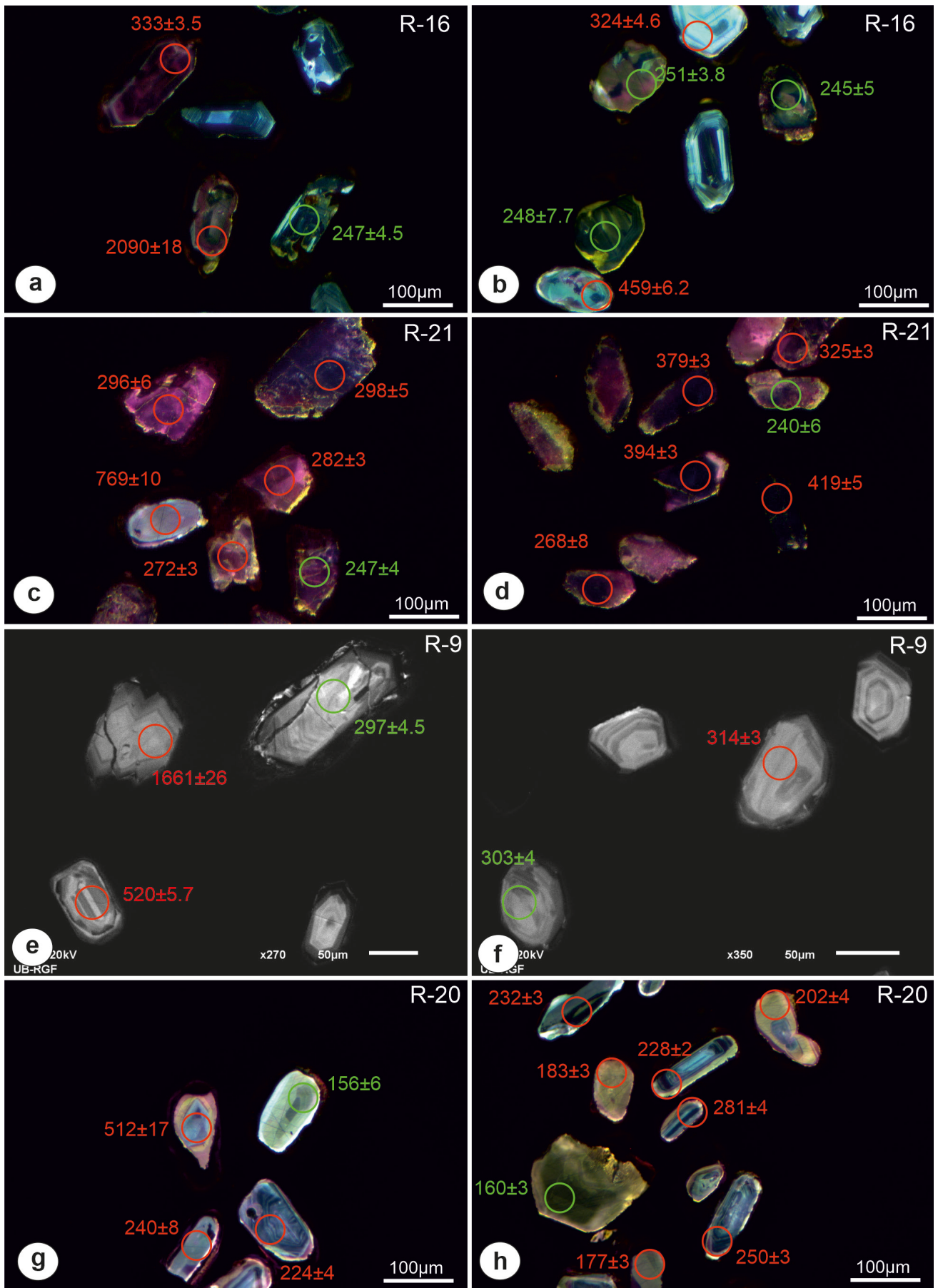
Fig. 4 - Selected cathodoluminescence images of dated zircons in meta-mafic rocks of the eastern Rhodope Massif. Circles represent the location of spot analyses with corresponding $^{206}Pb/^{238}U$ ages given with 2σ uncertainty. Point analyses in green were used for construction of age-defining concordia, while in red are point analyses in concordant inherited zircons.
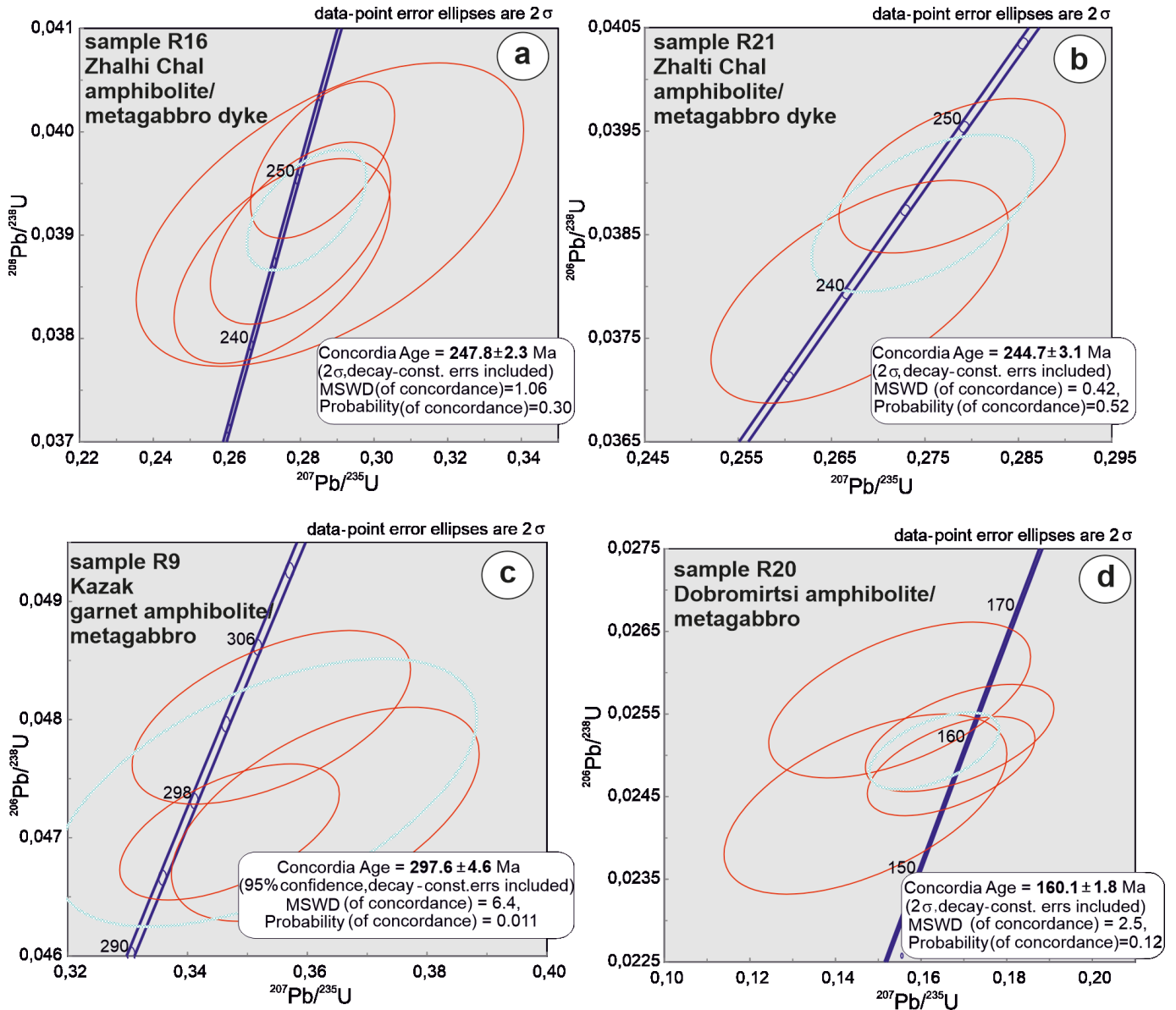
Fig. 5 - Concordia diagrams of U-Pb LA-ICP-MS zircon analyses of dated meta-mafic rock samples of the eastern Rhodope Massif.

eastern Rhodope Massif (e.g., Kozhoukharova, 1984b; 1999; Mposkos and Liati, 1993; Baziotis et al., 2008). Meta-gabbro dykes (samples R16 and R21) intruding the Zhalti Chal meta-ultramafic body display characteristic textures of microgabbro to coarse-grained gabbro, respectively, together with sample R20 of coarse-grained gabbro at the magmatic contact of Dobromirtsi body, whereas the garnet amphibolite sample R19 from the mafic dyke to the north of Kazak body and sample R9 at its contact are likely metamorphosed former basalts.

Our geochemical data, however, unequivocally reveal the magmatic nature of the studied meta-mafic rocks, i.e. the amphibolites, with gabbro-basalt protoliths. Major element composition demonstrates, low-K and high-Ti geochemical character of the analyzed meta-mafic rocks. The meta-mafic rocks are indistinguishable from MORB-type tholeiites in terms of their HFSE and REE abundances and HREE normalized patterns, in which they significantly overlap the N-MORB composition (Fig. 3). Thus, the geochemistry of the meta-mafic protoliths indicates their origin primarily from a depleted mantle source similar to MORB. This composi-

tional homogeneity of the meta-mafic rocks including magma type with MORB affinity, in turn, calls for the origin of their protoliths in an oceanic spreading ridge environment. However, some slight differences in the geochemistry of the studied samples can be deduced mainly in terms of the trace elements abundances. Sample R20 from Dobromirtsi body shows enrichment in some LILE such as Cs and Rb and an apparent high LILE/HFSE ratio that is usually attributed to arc-related petrogenesis (e.g., Pearce, 1982; 2008; Pearce et al 1984; McCuloch and Gamble, 1991; Tatsumi and Eggins, 1995). Other samples demonstrate a very weak elevation of the LILE/HFSE ratio.

In the Zhalti Chal meta-ultramafic body, the analyzed magmatic oscillatory zoned zircons yielded igneous crystallization U-Pb LA-ICP-MS ages of 247.8±2.3 Ma and 244.7±3.1 Ma, respectively, for the two gabbro dykes intruding the dunite-wehrlite. As both dykes postdate the crystallization of the meta-ultramafic body, they provide within the analytical error an Early Triassic minimum magmatic crystallization age ca. 250 Ma for the dunite-wehrlite, which is temporarily

very close to the Permian-Triassic boundary (251.902±0.024 Ma, ICS). Thus, these new crystallization ages define the end of the igneous evolution of the Zhalti Chal meta-ultramafic body in the very early beginning of the Triassic period. The crystallization age of the gabbroic protolith of the garnet amphibolites rimming the Kazak meta-ultramafic body at 297.6±4.6 Ma defines its Early Permian magmatic evolution. From the field relationships, the gabbro is intimately related to the Kazak meta-ultramafic body, and therefore, the gabbro represents the crustal portion in the magmatic "pseudostratig-raphy" of an ophiolite. Thus, the new crystallization ages outline the presence of distinct and different in age meta-ul-tramafic bodies that witnesses for an Early Permian and Early Triassic igneous evolution on the ocean floor. These igneous ages are further supported by the reported ages of ca. 298 Ma (Bauer et al., 2007) and 255-250 Ma (Liati et al., 2011) for the meta-mafic rocks in the upper high-grade basement unit of the eastern Rhodope Massif (see also Fig. 1a, 6c).

By contrast, the well-constrained new magmatic crystallization age of 160.1±1.8 Ma for the gabbro protolith of the amphibolite that rims the Dobromirtsi meta-ultramafic body unequivocally indicates the presence of a Late Jurassic mantle lithosphere fragment in the upper high-grade basement unit of the eastern Rhodope Massif. This Late Jurassic crystallization age of the gabbro protolith is close to the $^{40}Ar/^{39}Ar$ cooling age of 163.49±3.85 Ma of the Agriani gabbro from the Evros ophiolite of the low-grade Mesozoic unit and the crystallization age of 160.0±0.69 Ma of the meta-granite cross-cutting amphibolitized eclogite in the upper high-grade basement unit (Bonev et al., 2015). The latter age provides a Late Jurassic upper age limit for the igneous history of the gabbroic protolith of the amphibolitized eclogite.
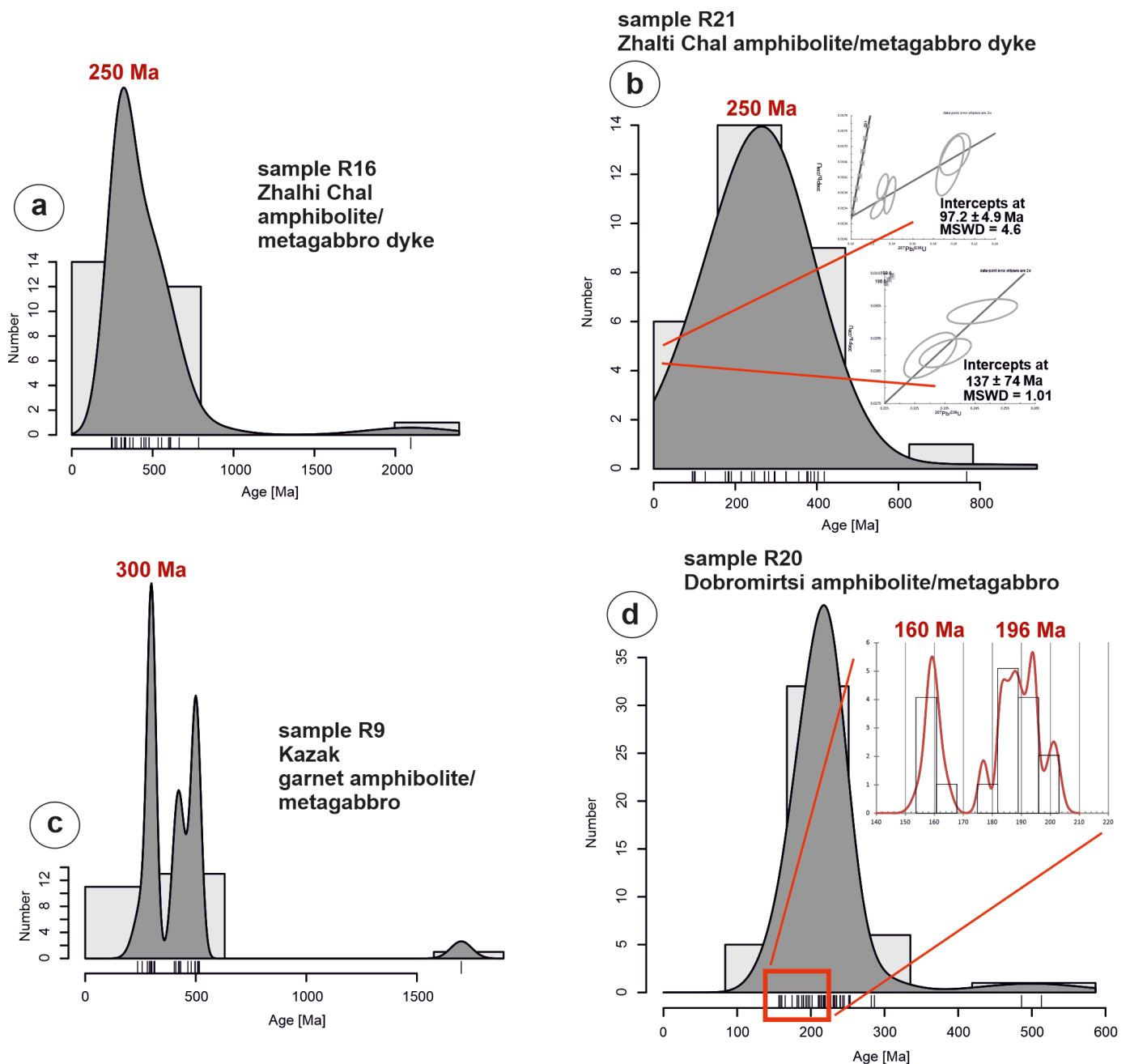

Fig. 6 - Kernel diagrams of U-Pb LA-ICP-MS zircon analyses of dated rock samples of the eastern Rhodope Massif. a) sample R16, b) sample R21, c) sample R9, d) sample R20.

The U-Pb geochronology yielded a range of ages older than the crystallization ages of the meta-mafic rock protoliths, including numerous concordant and discordant zircons (see Supplementary Table 1S, Fig. 6). Noteworthy, the ages of these virtually inherited zircons in the Zhalti Chal and Kazak bodies span mostly the entire Paleozoic, with only a few Proterozoic zircons. These inherited zircons fall within the age range of the known magmatic protoliths documented in both high-grade basement units of the eastern Rhodope Massif (Bonev et al., 2013a; 2015 and references therein). Contrary, the meta-mafic rocks at the Dodromirtsi body contain single Cambrian and Permian zircons, and mostly Triassic and Jurassic inherited zircons. Triassic granitoids are known in the Kesebir-Kardamos dome intruding both high-grade basement units (238-236 Ma-old Mt. Papikion pluton, Drakoulis et al., 2013), whereas Jurassic magmatic rocks (ca. 160-150 Ma) are known from the meta-granitoids in the upper high-grade basement unit (Cornelius, 2008; Liati et al., 2011; Bonev et al., 2015) and from the igneous members of the arc-related Evros ophiolite (Bonev et al., 2015). The age difference of inherited zircons in the Zhalti Chal and Kazak bodies (Paleozoic) and Dobromirtsi body (Triassic-Jurassic) implies a different crustal source area along the continental margins facing distinct in age oceanic lithosphere of the different oceanic basins.

In summary, the inherited zircons in the meta-mafic ophiolitic rocks demonstrate a complete picture of recycled older components from the continental margin of Eurasia represented by the units of the low- and high-grade crystalline basement of the eastern Rhodope Massif.

Tectonic implications

One of the existing tectonic interpretations relate the origin of the Rhodope meta-ultramafic ophiolite bodies to Precambrian formation and obduction of the oceanic crust onto former active at that time margin (Kozhoukharova, 1984a). Other links the eastern Rhodope meta-ophiolites, together with the Volvi meta-ophiolites, to the Triassic-Jurassic ocean floor formation and pre-Late Jurassic obduction onto the Eurasian plate margin in the Tethyan realm (Papanikolaou, 2009; 2013). The latter interpretation is partly close to the radiometric dates obtained in this study for the eastern Rhodope meta-ultramafic ophiolite bodies. This is because the Volvi meta-ophiolites, which were considered as an element of the Paleotethys Ocean suture (Şengör et al., 1984), have been proven as the Neotethyan Middle Triassic (ca. 240 Ma) rift-related continental margin ophiolite (Bonev et al., 2019b). In this way the Triassic rift-related magmatic bodies of the Serbo-Macedonian-Rhodope massifs demonstrate close compositional and temporal similarity to mantle-derived Triassic mafic to evolved rift-related units documented in the Alps as a follow up of the Pangea break-up (e.g., Casetta et al., 2018; 2019; De Min et al., 2020; Storck et al., 2020).

Most of the paleotectonic reconstructions and geodynamic models for the Tethyan realm invariably have shown that the Paleotethys was the mid- to late Paleozoic ocean that ultimately closed by the end of Triassic time following the subduction under the Eurasian continental margin (Şengör et al., 1984; Robertson and Dixon, 1984; Robertson et al., 1996; Stampfli, 2000; Stampfli and Borel, 2002; Stampfli et al., 2013; Okay and Topuz, 2017). Paleotethys Ocean subduction has created voluminous Late Carboniferous-Permian to Middle Triassic continental magmatic arc on the upper plate represented by the Eurasian active continental margin,

including the Serbo-Macedonian and Rhodope massifs and the Sakar-Strandzha zone (see Fig. 1a, inset; Peytcheva et al., 2004; Turpaud and Reischmann, 2010; Himmerkus et al., 2012; Bonev et al., 2022). The paleotectonic reconstructions of the Mediterranean Tethys (e.g., Stampfli and Borel, 2002) have also shown Middle-Late Triassic back-arc basin openings along the Eurasian plate margin as a result of the Paleotethys oceanic subduction and final closure, following the Late Permian-Triassic rifting phase. In the eastern Mediterranean region, this rifting phase created the Küre, Pindos, Meliata and Maliac oceanic basins (the latter relevant to the region studied here), whose subsequent seafloor spreading span from the Middle Triassic to Early Jurassic time (e.g., Robertson, 2002; Stampfli and Kozur, 2006; Stampfli and Hochard, 2009; Ferrière et al., 2016).

Based on MORB affinity displayed by the studied meta-mafic rocks tightly connected to the meta-ultramafic bodies of similar affinity (Kolcheva and Eskenazy, 1988; Kolcheva et al., 2000), the upper high-grade basement unit of the eastern Rhodope Massif unequivocally contains remnants of the Tethyan oceanic lithosphere, which visibly belongs to different Tethyan oceans, namely Paleotethys and Neotethys as deduced from the ages obtained by U-Pb geochronology in this study.

On account of the regional geology, geochemistry, and ages of the studied meta-mafic rocks, we can propose a tectonic scenario for the crustal interaction at the Eurasian plate margin of Tethyan seaways oceanic lithosphere (Fig. 7). The key characteristics of the meta-ultramafic bodies in the central Byala reka dome is their different age, which encompasses in three district bodies Late Devonian, Early Permian and Early Triassic mantle lithosphere remnants. The central Byala reka dome meta-ultramafic bodies fall in the temporal frame of the Paleotethys ocean floor widening and subsequent consumption by subduction. Another important feature is the occurrence of the meta-ultramafic bodies in the central Byala reka dome, together and coupled with the sedimentary host rocks such as the enveloping various mica schists. The different age of the meta-ultramafic bodies hosted by meta-sedimentary rocks calls for a mélange, which easily can be related to the subduction-accretion history of the aforementioned rock assemblage. We interpret Late Devonian to Early Triassic meta-ultramafic bodies and host meta-sedimentary rocks as telescoped in an accretionary mélange during the subduction of the Paleotethys oceanic lithosphere under and along the Eurasian plate margin (Fig. 7a). Maximum age of the accretion of the mélange to the continental margin is envisaged during the Middle Triassic judging from the emplacement of ca. 236 Ma-aged Mt. Papikion granitoids in the upper high-grade basement unit (see Fig. 1a), which fits temporarily the pre-Jurassic final closure of the Paleotethys ocean. It is therefore highly probable that the aforementioned mélange might well represents an element of the Paleotethys suture, which however was highly reworked during the Alpine tectono-metamorphic processes.

The Late Jurassic age of the meta-gabbro at the contact of Dobromirtsi meta-ultramafic body calls for the presence of Neotethys Ocean mantle lithosphere remnant, and thus offers an opportunity to test the hypothesis for hidden mantle section of the Jurassic Evros ophiolite from the low-grade Mesozoic unit within the upper high-grade basement unit of the eastern Rhodope Massif. Indeed, there, recently a meta-gabbro at the village of Bubino yields a Late Jurassic age at 166 Ma for the crystallization of the protolith (Filipov et al., 2022), but the meta-gabbro is not directly connected to ultra-mafic body.
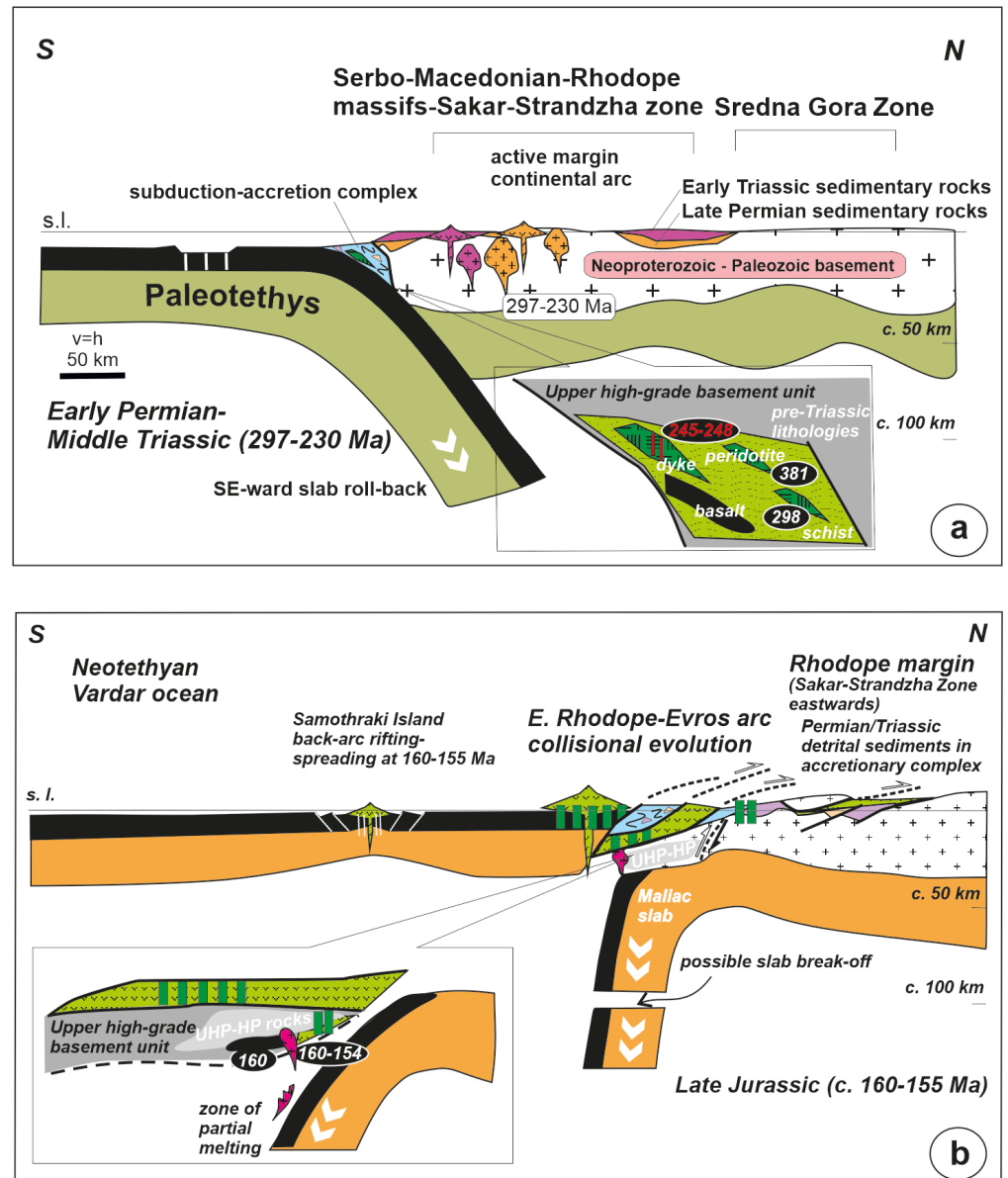
Fig. 7 -a) Tectono-magmatic scenario for the Permian-Triassic continental arc-related magmatism at active continental margin of Eurasia represented by the Sakar-Strandzha Zone, Serbo-Macedonian and Rhodope massifs (modified after Bonev et al., 2022). b) Tectono-magmatic scenario for the Late Jurassic tectonic emplacement of the Evros ophiolite (modified after Bonev et al., 2015).

The supra-subduction zone Early-Middle Jurassic Evros ophiolite is related to the interaction of the Maliac oceanic basin and Neotethyan Vardar Ocean (Bonev and Stampfli, 2003; 2011; Bonev et al., 2015). Following Late Permian-Triassic rifting and Triassic spreading, the Maliac Ocean basin developed as the Main Vardarian Tethyan Ocean basin during the Jurassic, with its Pelagonian (western) and the Serbo-Macedonian-Rhodope (eastern) continental margins (Ferrière and Stais, 1995; Ferrière et al., 2016). From Mid-Late Jurassic times onward the Maliac oceanic basin was totally replaced by the Neotethyan Vardar oceanic basin in the sense of Stampfli and Borel (2002), Bonev and Stampfli (2003; 2011), Stampfli and Hochard (2009) and Bonev et al. (2015), in which interpretation the intra-oceanic subduction of the Maliac oceanic lithosphere established the Evros ophiolite on the Vardarian upper plate. It becomes evident from the density distribution of the ages that the gabbroic protolith at the Dobromitrtsi body contains Early to Late Jurassic (peaked at 160 Ma and 196 Ma) lithosphere components temporally encompassing the timing of interaction between the Maliac and Vardar oceanic basins (Fig. 6d).

The age of 160.1±1.8 Ma for the meta-gabbro at Dobromirtsi is close within the analytical error to the cooling age of 163.49± 385 Ma for the Agriani gabbro from the Evros ophiolite (Bonev et al., 2015) and approximately coincides with the age of 161 Ma of the youngest detrital zircon in the sedimentary rocks associated with this ophiolite in the low-grade Mesozoic unit (Meinhold et al., 2010) (see Fig. 1a). The consistency of above ages, including the Dobromirtsi meta-gabbro, indicates that the Dobromirtsi ultra-mafic body temporarily represents an integral part of the mantle section of the Evros ophiolite, and thus Dobromirtsi meta-ophiolite testifies for the presence of a Late Jurassic Neotethys Ocean mantle lithosphere in closer proximity to the Rhodope margin of Eurasia (Fig. 7b). The low-grade Mesozoic unit, including the Evros ophiolite, was tectonically emplaced onto the upper high-grade basement unit via subduction-accretion processes in Late Jurassic times ca. 157-154 Ma (Bonev et al., 2010b, 2015) before the deposition of the Early Cretaceous limestone (Ivanova et al., 2015) that seals this tectonic event.

CONCLUSIONS

Our results for the eastern Rhodope Massif meta-ophiolites highlight the following critical points for the Paleozoic and Mesozoic ocean floor igneous history and tectonic interaction at the Eurasian plate margin.

(i) In the eastern Rhodope Massif, the studied meta-mafic ophiolitic rocks show trace element and REE compositions demonstrating a MORB-type geochemical signature, which have been emplaced as posterior cross-cutting gabbro dykes and concomitant gabbro-basalt layers connected to three meta-ultramafic bodies as indicated by the field data. The geochemical signature of the meta-mafic ophiolitic rocks is similar to the geochemical affinity of the meta-ultramafic bodies and consistent with origin in an oceanic spreading ridge tectonic environment.

(ii) U-Pb geochronology reveals the Early Triassic crystallization age of the gabbro dykes, which is a minimum igneous age for the Zhalti Chal meta-ultramafic ophiolitic body. The amphibolite at the rim of a second, Kazak meta-ultramafic body has Early Permian crystallization age of the basaltic protolith. The amphibolite at the rim of the third, Dobromirtsi meta-ultramafic body has Late Jurassic crystallization age of the gabbroic protolith. Thus, these new U-Pb zircon ages reveal the presence of hidden previously unknown Late Paleozoic and Mid-Mesozoic mantle components of oceanic lithosphere represented by the meta-ultramafic bodies in the upper high-grade basement unit of the eastern Rhodope Massif. Interestingly, the U-Pb geochronology reveals a main cluster of Paleozoic inherited zircons in the meta-mafic rocks with Early Permian and Early Triassic magmatic ages, while the Late Jurassic meta-mafic rocks have a main cluster of Triassic and Jurassic inherited zircons, which suggest a provenance from a different time-integrated crustal source of the adjacent continental margin.

(iii) The meta-ultramafic bodies have different ages, which encompass the aforementioned Permian and Triassic bodies and another spatially close Late Devonian body, all testifying for mantle lithosphere remnants that fall in the temporal frame of the Paleotethys ocean floor development and subsequent closure by subduction. As the different in age meta-ultramafic bodies are hosted by enveloping mica schists, this occurrence calls for a mélange related to the subduction-accretion history of the whole rock assemblage. Late Devonian to Early Triassic meta-ultramafic bodies and host meta-sedimentary rocks are telescoped in an accretionary mélange during the subduction of the Paleotethys oceanic lithosphere under the Eurasian plate margin. The maximum age of the accretion of the mélange to the Eurasian continental margin is envisaged during the Middle Triassic, which fits the pre-Jurassic closure of the Paleotethys Ocean. The mélange might well represent an element of the Paleotethys suture, which was strongly reworked during the Alpine tectono-metamorphic processes.

(iv) The Late Jurassic age of the MORB-type meta-gabbro at the contact of Dobromirtsi meta-ultramafic body in turn calls for the presence of Neotethys Ocean mantle lithosphere remnant, and is therefore a test for the hypothesis about hidden mantle section of the Jurassic Evros ophiolite from the low-grade Mesozoic unit within the upper high-grade basement unit of the eastern Rhodope Massif. The answer to this hypothesis is positive, and supported by Jurassic crystallization ages of the Evros ophiolite and related Jurassic detrital zircon record in low-grade Mesozoic unit sedimentary successions, together with the Late Jurassic tectonic emplacement history of the latter unit on top of the upper high-grade basement unit.

Supplementary Material

Supplementary data associated with this article can be found in the online version at https://ofioliti.it/index.php/ofioliti/article/view/717

REFERENCES

Bauer C., Rubatto D., Krenn K., Proyer A. and Hoinkes G., 2007. A zircon study from the Rhodope metamorphic complex, N-Greece: Time record of a multistage evolution. Lithos, 99: 207-228.

Baziotis I., Mposkos E. and Perdikatsis V., 2008. Geochemistry of amphibolitized eclogites and cross-cutting tonalitic-trondhjemitic dykes in the Metamorphic Kimi Complex in East Rhodope (N.E. Greece): implications for partial melting at the base of a thickened crust. Intern. J. Earth Sci., 97: 459-477.

Baziotis I., Mposkos E. and Asimow P.D. 2014. Continental rift and oceanic protoliths of mafic-ultamafic rocks from the Kechros Complex, NE Rhodope (Greece): implications from petrography, major and trace-element systematics and MELTS modeling partial melting at the base of a thickened crust. Intern. J. Earth Sci., 103: 981-1003.

Bazylev B.A., Zakariadze G.S., Zeljazkova-Panayotova M.D., Kolcheva K., Obërhansli R. and Solovieva N.V., 1999. Petrology of ultrabasites from the ophiolitic association in crystalline basement of the Rhodope Massif. Petrology, 7: 191-212. (in Russian)

Bonev N., 2006. Cenozoic tectonic evolution of the eastern Rhodope Massif (Bulgaria): basement structure and kinematics of syn- to postcollisional extensional deformation. In: Y. Dilek and S. Pavlides (Eds.), Post-collisional tectonics and magmatism in the Mediterranean Region and Asia. Geol. Soc. Am. Spec. Paper, 409: 211-235.

Bonev N., 2015. Protoliths and metamorphic events in the high-grade metamorphic basement of the Eastern Rhodope: constraints from U-Pb zircon geochronology. Proc. Ann. Conf. Bulg. Geol. Soc. "Geosciences 2015", pp. 57-58.

Bonev N. and Beccaletto L., 2007. From syn- to post-orogenic Tertiary extension in the north Aegean region: constraints on the kinematics in the eastern Rhodope-Thrace, Bulgaria-Greece and the Biga Peninsula, NW Turkey, In: T. Taymaz, Y.Yilmaz and Y. Dilek (Eds.), The Geodynamics of the Aegean and Anatolia. Geol. Soc. London Spec. Publ., 291: 113-142.

Bonev N. and Stampfli G.M., 2003. New structural and petrologic data on Mesozoic schists in the Rhodope (Bulgaria): geodynamic implications. C.R. Geosci., 335: 691-699.

Bonev N. and Stampfli G., 2008. Petrology, geochemistry and geodynamic implications of Jurassic island arc magmatism as revealed by mafic volcanic rocks in the Mesozoic low-grade sequence, eastern Rhodope, Bulgaria. Lithos, 100: 210-233.

Bonev N. and Stampfli G. 2009. Gabbro, plagiogranite and associated dykes in the supra-subduction zone Evros ophiolites, NE Greece. Geol. Mag., 146: 72-91.

Bonev N. and Stampfli G., 2011. Alpine tectonic evolution of a Jurassic subduction-accretionary complex: deformation, kinematics and [40]Ar/[39]Ar age constraints on the Mesozoic low-grade schists of the Circum-Rhodope belt in the eastern Rhodope-Thrace region, Bulgaria-Greece. J. Geodyn., 52: 143-167.

Bonev N., Burg J.-P. and Ivanov Z., 2006. Mesozoic-Tertiary structural evolution of an extensional gneiss dome - the Kesebir-Kardamos dome, eastern Rhodope (Bulgaria-Greece). Intern. J. Earth Sci., 95: 318-340.

Bonev N., Dotseva Z. and Filipov P., 2023. Geochemistry and tectonic significance of metamorphosed mafic ophiolitic rocks in the high-grade metamorphic basement of the eastern Rhodope Massif (Bulgaria-Greece). Geol. Carpath., 74: 23-39.

Bonev N., Filipov P., Raicheva R. and Moritz R., 2019a. Timing and tectonic significance of Paleozoic magmatism in the Sakar unit of the Sakar-Strandzha Zone, SE Bulgaria. Intern. Geol. Rev., 61, 16: 1957-1979.

Bonev N., Filipov P., Raicheva R. and Moritz R., 2022. Evidence of late Paleozoic and Middle Triassic magmatism in the northern-western Sakar-Strandzha Zone, SE Bulgaria: Regional geodynamic implications. Intern. Geol. Rev., 64: 1199-1225.

Bonev N., **M**agganas A. and Klain L., 2010a. Regional geology and correlation of the eastern Circum-Rhodope Belt, Bulgaria-Greece. Sci. Ann. School Geol., Aristotle Univ. Thessaloniki, Proc. 19th Congr. CBGA, Spec. Vol. 100: 157-164.

Bonev N., Marchev P., Moritz, R. and Collings D., 2015. Jurassic subduction zone tectonics of the Rhodope Massif in the Thrace region (NE Greece) as revealed by new U-Pb and ^{40}Ar/^{39}Ar geochronology of the Evros ophiolite and high-grade basement rocks. Gondw. Res., 27: 760-775.

Bonev N., Ovtcharova-Schaltegger M., Moritz R., Marchev P. and Ulianov A., 2013a. Peri-Gondwanan Ordovician crustal fragments in the high-grade basement of the Eastern Rhodope Massif, Bulgaria: evidence from U-Pb LA-ICP-MS zircon geochronology and geochemistry. Geodin. Acta, 26: 207-229.

Bonev N., Moritz R., Borisova M. and Filipov P., 2019b. Therma-Volvi-Gomati complex of the Serbo-Macedonian Massif, Northern Greece: A Middle Triassic continental margin ophiolite of Neotethyan origin. J. Geol. Soc. London, 176: 931-944.

Bonev N., Spikings R., Mortiz R. and Marchev P., 2010b. The effect of early Alpine thrusting in late-stage extensional tectonics: Evidence from the Kulidzhik nappe and the Pelevun extensional allochthon in the Rhodope Massif, Bulgaria. Tectonophysics, 488: 256-281.

Bonev N., Spikings R., Moritz R., Marchev P. and Collings D., 2013b. ^{40}Ar/^{39}Ar age constraints on the timing of Tertiary crustal extension and its temporal relation to ore-forming and magmatic processes in the eastern Rhodope Massif, Bulgaria. Lithos, 180-181: 264-278.

Boyanov I. and Goranov A., 2001. Late Alpine (Paleogene) superimposed depressions in parts of southeastern Bulgaria. Geol. Balc., 31: 3-36.

Boyanov I., Ruseva M., Toprakcieva V. and Dimitrova E., 1990. Lithostratigraphy of the Mesozoic rocks from the Eastern Rhodopes. Geol. Balc. 20, 3-28. (in Russian)

Brun J-P. and Sokoutis D., 2018. Core complex segmentation in North Aegean, a dynamic view. Tectonics, 37: 1797-1830.

Burg J.-P., 2012. Rhodope: From Mesozoic convergence to Cenozoic extension. Review of petro-structural data in the geochronological frame. In: E. Skourtsos, G.S. Lister (Eds.), Geology of Greece., J. Virt. Expl. 42, paper 1, doi: 10.3809/jvirtex.2011.00270

Burg J-P., Ricou L-E., Ivanov Z., Godfriaux I., Dimov D. and Klain L., 1996. Syn-metamorphic nappe complex in the Rhodope Massif. Structure and kinematics. Terra Nova, 8: 6-15.

Carrigan C.W., Mukasa S.B., Haydoutov I. and Kolcheva K., 2003. Ion microprobe U-Pb zircon ages of pre-Alpine rocks in the Balkan, Sredna Gora and Rhodope terranes of Bulgaria: constraints on Neoproterozoic and Variscan tectonic evolution. J. Czech Geol. Soc., 48: 32-33.

Casetta F., Coltorti M., Ickert R.B., Bonadiman C., Giacomoni P.P. and Ntaflos T. 2018. Intrusion of shoshonitic magmas at shallow crustal depth: T-P path, H$_2$O estimates, and AFC modeling of the Middle Triassic Predazzo Intrusive Complex (Southern Alps, Italy). Contrib. Miner. Petr., 173: 57.

Casetta F., Ickert R.B., Mark D.F., Bonadiman C., Giacomoni P.P., Ntaflos T. and Coltorti M. 2019. The Alkaline Lamprophyres of the Dolomitic Area (Southern Alps, Italy): Markers of the Late Triassic change from orogenic-like to anorogenic magmatism. J. Petrol., 60: 1263-1298.

Chen X., Sun X., Wu Z., Wang Y., Lin X. and Chen H., 2021. Mineralogy and geochemistry of deep-sea sediments from the ultraslow-spreading southwest Indian ridge: Implications for hydrothermal input and igneous host rock. Minerals, 11: 138.

Christofides G., Koroneos A., Soldatos T., Eleftheriadis G. and Kilias A., 2001. Eocene magmatism (Sithonia and Elatia plutons) in the internal Hellenides and implications for Eocene-Miocene geological evolution of the Rhodope Massif (Northern Greece). Acta Vulcanol., 13: 73-89.

Christofides G., Peckay Z., Elefteriadis G., Soldatos T. and Koroneos A., 2004. The Tertiary Evros volcanic rocks (Thrace, northernmost Greece): petrology and K/Ar geochronology. Geol. Carpath., 55: 397-409.

Cornelius N.K., 2008. UHP metamorphic rocks from the Eastern Rhodope Massif, NE Greece: new constraints from petrology, geochemistry and zircon ages. Ph.D. thesis, , Univ. Mainz, Germany., 173 pp.

De Min A., Velicogna M., Ziberna L., Chiaradia M., Alberti A. and Marzoli A., 2020. Triassic magmatism in the European Southern Alps as an early phase of Pangea break-up. Geol. Mag, 157:1800-1822.

Del Moro A., Innocenti F., Kyriakopoulos C., Manetti P. and Papadopoulos P., 1988. Tertiary granitoids from Thrace (northern Greece): Sr isotopic and petrochemical data. N. Jahrb. Geol. Paläontol. Abh., 159: 113-135.

Dinter D.A., 1998. Late Cenozoic extension of the Alpine collisional orogen, northeastern Greece: Origin of the north Aegean basin. Geol. Soc. Am. Bull., 110: 1208-1230.

Dinter D.A. and Royden L., 1993. Late Cenozoic extension in northeastern Greece: Strymon Valley detachment system and Rhodope metamorphic core complex. Geology, 21: 45-48.

Dinter D.A., Macfarlane A.M., Hames W., Isachsen C., Bowring S. and Royden L., 1995. U-Pb and ^{40}Ar/^{39}Ar geochronology of the Symvolon granodiorite: implications for the thermal and structural evolution of the Rhodope metamorphic core complex, northeastern Greece. Tectonics, 14: 886-908.

Drakoulis A., Koroneos A., Poli G., Soldatos T., Papadopoulou L., Murata M. and Eliwa H., 2013. U-Pb zircon dating of the Mt. Papikon pluton (central Rhodope, Greece): new constraints on the evolution of Kesebir-Kardamos dome. Acta Vulcanol., 25: 83-98.

Ferrière J. and and Stais A., 1995. Nouvelle interprétation de la suture téthysienne vardarienne d'après l'analyse de série de Péonias (Vardar oriental, Hellénides internes). Bull. Soc. Géol. Fr., 166 (4): 327-339.

Ferrière J., Baumgartner P.O. and Chanier F., 2016. The Maliac Ocean: the origin of Tethyan Hellenic ophiolites. Intern. J. Earth Sci., 105: 1941-1963.

Filipov P., Ichev M., Bonev N., Georgiev S. and Dotseva Z., 2022. LA-ICP-MS U-Pb zircon age of amphibolite protoliths associated with metaophiolites near the villages of Dobromirtsi and Bubino, east Rhodopes, Bulgaria. 22th Congr. CBGA, Abstr. Book, Geol. Balc., p. 275.

Froitzheim N., Jahn-Ave S., Frei F., Wainwright A.N., Maas R., Georgiev N., Nagel T.J. and Pleuger J., 2014. Age and composition of meta-ophiolite from the Rhodope Middle Allochthon (Satovcha, Bulgaria): A test for maximum-allochthony hypothesis of the Hellenides. Tectonics, 32: 1477-1500, doi:10.1002/2014TC003526.

Harkovska A., Yanev Y. and Marchev P., 1989. General features of the Paleogene orogenic magmatism in Bulgaria. Geol. Balcan., 19: 37-72.

Haydoutov I., Kolcheva K., Daieva L.A, Savov I. and Carrigan C.W., 2004. Island arc origin of the variegated formations from the east Rhodope, Bulgaria - implications for the evolution of the Rhodope massif. Ofioliti. 29: 145-157.

Himmerkus F., Zachariadis P., Reischmann T. and Kostopoulos D., 2012. The basement of the Mount Athos Peninsula, northern Greece: insights from geochemistry and zircon ages. Intern. J. Earth Sci., 101: 1467-1485.

16

Innocenti F., Kolios N., Manetti P., Mazzuoli R., Peccerillo A., Rita F. and Villari L., 1984. Evolution and geodynamic significance of Tertiary orogenic volcanism in northeastern Greece. Bull. Vulcanol., 47: 25-37.

Ivanov R. and Kopp K.O., 1969. Das Alttertiär Thrakiens und der Ostrhodope. Geol. Paleontol., 3: 123-153.

Ivanova D., Bonev N. and Chatalov, A., 2015. Biostratigraphy and tectonic significance of lowermost Cretaceous carbonate rocks of the Circum-Rhdope Belt (Chalkidiki Peninsula and Thrace region, NE Greece). Cret. Res., 52: 25-63.

Jackson S.E., Pearson N.J., Griffin W.L. and Belousova E.A., 2004. The application of laser ablation-inductively coupled plasma-mass spectrometry to in situ U–Pb zircon geochronology: Chem. Geol., 211: 47-69.

Kauffmann G., Kockel F. and Mollat H., 1976. Notes on the stratigraphic and paleogeographic position of the Svoula formation in the Innermost Zone of the Hellenides (Northern Greece). Bull. Soc. Géol. Fr., 18: 225-230.

Kelemen P.B., Hanghoj K. and Greene A.R., 2014. One view of the geochemistry of subduction-related magmatic arcs, with an emphasis on primitive andesite and lower crust. In: H.D. Holland. and Turekian K.K. (Eds.), Treatise on Geochemistry, Elsevier, 4: 749-805.

Kolcheva K. and Eskenazy G., 1988. Geochemistry of metaeclogites from the Central and Eastern Rhodope Mts (Bulgaria). Geol. Balc., 18: 61-78.

Kolcheva K., Haydoutov I., and Daieva L., 2000. Dismembered ultramafic ophiolites from the Avren synform, Eastern Rhodopes. Geochem. Miner. Petrol. (Sofia), 37: 27-38.

Koukouvelas I. and Doutsos T., 1990. Tectonic stages along a traverse cross-cutting the Rhodopian zone (Greece). Geol. Rundsch., 79: 753-776.

Kozhoukharov D., Kozhoukharova E.and Papanikolaou D., 1988. Precambrian in the Rhodope massif. In: V. Zoubek, J. Cogné, D. Kozhoukharov and H.G. Kräutner (Eds.), Precambrian in younger fold belts - European Variscides, the Carpathians and Balkans. John Willey and Sons, Chichester, p. 723-778.

Kozhoukharov, E., 1984a. Origin and structural position of the serpentinized ultrabasic rocks of the Precambrian ophiolitic association in the Rhodope Massif. I. Geologic position and composition of ophiolite association. Geol. Balc., 14: 9-36.

Kozhoukharova E., 1984b. Origin and structural position of the serpentinized ultrabasic rocks of the Precambrian ophiolitic association in the Rhodope Massif. II. Metamorphic alteration of ultrabasics. Geol. Balc.,14: 3-35.

Kozhoukharova E., 1999. Metasomatic gabbroids-markers in the tectono-metamorphic evolution of the Eastern Rhodopes. Geol. Balc., 29: 89-109.

Liati A., 2005. Identification of repeated Alpine (ultra) high-pressure metamorphic events by U-Pb SHRIMP geochronology and REE geochemistry of zircon: the Rhodope zone of Northern Greece. Contrib. Miner. Petrol., 150: 608-630.

Liati A. and Mposkos E., 1990. Evolution of eclogites in the Rhodope zone of northern Greece. Lithos, 25: 89-99.

Liati A., Gebauer D. and Fanning C.M., 2011. Geochronology of the Alpine UHP Rhodope zone: A review of isotopic ages and constraints on the geodynamic evolution. In: L.F. Dobrzhinetskaya, S.W. Faryad, S.Wallis and S. Cuthbert (Eds.), Ultrahigh-pressure metamorphism 25 Years after the discovery of Coesite and Diamond. Elsevier, pp. 295-324.

Lips A.L.W., White S.H. and and Wijbrans J.R., 2000. Middle-Late Alpine thermotectonic evolution of the southern Rhodope Massif, Greece. Geodin. Acta, 13: 281-292.

Ludwig K.R., 2011. User's Manual for Isoplot/Ex, Version 4.15. A Geochronological Toolkit for Microsoft Excel. Berkeley Geochron. Center Spec. Publ., 4: 2455, Berkeley.

Magganas A.C., 2002. Constraints on the petrogenesis of Evros ophiolite extrusives, NE Greece. Lithos, 65: 165-182.

Marchev P., Georgiev S., Raicheva R., Peytcheva I., von Quadt A., Ovtcharova M. and Bonev N., 2013. Adakitic magmatism in post-collisional setting: An example from the Early-Middle Eocene magmatic belt in South Bulgaria and North Greece. Lithos, 180-181: 159-180.

Marchev P., Kibarov P., Spikings R., Ovtcharova M., Márton I. and Moritz R., 2010. $^{40}Ar/^{39}Ar$ and U-Pb geochronology of the Iran Tepe volcanic complex, Eastern Rhodopes. Geol. Balc., 39: 3-12.

Marchev P., von Quadt A., Peytcheva I. and Ovtcharova M., 2006. The age and origin of the Chuchuliga and Rozino granites, Eastern Rhodopes. Proc. Ann. Conf. Bulg. Geol. Soc. "Geosciences 2006, p. 13-216.

McCulloch M.T. and Gambl, J.A., 1991. Geochemical and geodynamical constraints on subduction zone magmatism. Earth Planet. Sci. Lett., 102: 358-374.

McDonough W.F. and Sun S.S., 1995. The composition of the Earth. Chem. Geol. 120: 223-253.

Meinhold G. and Kostopoulos D., 2013. The Circum-Rhodope Belt, northern Greece: Age, provenance, and tectonic setting. Tectonophysics, 595-596: 55-68.

Meinhold G., Reischmann T., Kostopoulos D., Frei D. and Larionov A.N., 2010. Mineral chemical and geochronological constraints on the age and source of the eastern Circum-Rhodope Belt low-grade metasedimentary rocks, NE Greece. Sedim. Geol., 229: 207-233.

Meyer W., 1968. Alterstellung des plutonismus im Sdteil der Rila-Rhodope-Masse. Geol. Paleont.,2: 177-192.

Mposkos E.D. and Kostopoulos D.K., 2001. Diamond, former coesite and supersilicic garnet in metasedimentary rocks from the Greek Rhodope: a new ultrahigh-pressure metamorphic province established. Earth Planet. Sci. Lett., 192: 497-506.

Mposkos E.D. and Liati A., 1993. Metamorphic evolution of metapelites in the high-pressure terrane of the Rhodope zone, northern Greece. Can. Miner., 31: 401-424.

Mposkos E. and Perdikatsis B., 1989. Eclogite-amphibolites in the east Rhodope. Geol. Rhodop., 1:160-168.

Mposkos E., Baziotis I. and Proyer A., 2012. Pressure-temperature evolution of eclogites from the Kechros complex in the Eastern Rhodope (NE Greece). Int. J. Earth Sci., 101: 2083-2099.

Mposkos E., Perdikatsis B. and Liati A., 1989. Geochemical investigation of amphibolites from eastern and central Rhodope. Bull. Geol. Soc. Greece, 23: 413-425.

Nikolaev G., 1958. Geology of the surroundings of the villages Benkovski and Dragovo, Momchilgrad area. Ann. Inst. Mining Geol., 4: 25-54.

Okay A.I. and Topuz G., 2017. Variscan orogeny in the Black Sea region. Intern. J. Earth Sci., 106: 569-592.

Ovtcharova M., von Quadt A., Heinrich C.A., Frank M., Kaiser-Rohmeier M., Peycheva I. and Cherneva Z., 2003. Triggering of hydrothermal ore mineralization in the Central Rhodopean Core Complex (Bulgaria)-insight from isotope and geochronological studies on tertiary magmatism and migmatisation. In: Eliopoulos et al. (Eds.), Miner. Explor. Sustainable Developm., 1: 367-370. Millpress, Rotterdam.

Papadopoulos P., Arvanitidis N. and Zanas I., 1989. Some preliminary geological aspects on the Makri unit (Phyllite series), Peri-Rhodope Zone. Geol. Rhodop., 1:34-42.

Papanikolaou D., 2009. Timing of tectonic emplacement of the ophiolites and terrane paleogeography in the Hellenides. Lithos, 108: 262-280.

Papanikolaou D., 2013. Tectonostratigraphic models of the Alpine terranes and subduction history of the Hellenides. Tectonophysics, 595-596: 1-24.

Paton C., Hellstrom J., Paul B., Woodhead J. and Hergt J., 2011. Iolite: freeware for the visualization and processing of mass spectrometric data. J. Analyt. Atomic Spectr., 26: 2508-2518.

Payakov I., Zheliazkova-Panayotova M. and Ivchinova L., 1963. Structural-textural features and mineral composition of chromite ores of Dobromirtsi deposit. Ann. Sofia Univ. Fac. Biol. Geol. Geogr., 56: 219-251.

Pearce J.A., 1982. Trace element characteristics of lavas from destructive plate boundaries. In: R.S. Thorpe (Ed.), Andesites: orogenic andesites and related rocks. John Wiley and Sons, Chichester, p. 525-548.

Pearce J.A., 2008. Geochemical fingerprinting of oceanic basalts with applications to ophiolite classification and the search for Archean oceanic crust. Lithos, 100: 14-48.

Pearce J.A., Lippard S.J. and Roberts S., 1984. Characteristics and tectonic significance of supra-subduction zone ophiolites. In: B.P. Kokelaar and M.F. Howells (Eds.), Marginal Basin geology: volcanic and associated sedimentary and tectonic processes in modern and ancient marginal basins. Geol. Soc. London Spec. Publ., 16: 77-94.

Pe-Piper G. and Piper D.J.W., 2002. The igneous rocks of Greece. The anatomy of an orogen. Gebrueder Borntraeger, Berlin-Stuttgart, pp. 573.

Peytcheva I. and von Quadt A., 1995. U-Pb zircon dating of metagranites from Byala Reka region in the east Rhodopes, Bulgaria. In: D. Papanikolaou (Ed.), Proceed. 15th Congr. CBGA, Geol. Soc. Greece Spec. Publ., 4: 637-642.

Peytcheva I., von Quadt A., Machev, L., Kolcheva K. and Sarov S., 2018. Relics of Devonian oceanic lithosphere in Byala Reka dome, Eastern Rhodopes: Evidence from zircon U-Pb dating and Hf-isotope tracing. C.R. Acad. Bulg. Sci.. 71: 1657-1664.

Peytcheva I., Von Quadt A., Ovtcharova M., Handler R., Neubauer F., Salnikova E., Kostitsin Y., Sarov S.. and Kolcheva K., 2004. Metagranitoids from the eastern part of the Central Rhodopean Dome (Bulgaria): U-Pb, Rb-Sr and ^{40}Ar/^{39}Ar timing of emplacement and isotopic-geochemical features. Miner. Petrol., 82: 1-31.

Plank T., 2014. The chemical composition of subducting sediments, In: H.D. Holland (Ed.), Treatise on Geochemistry. Elsevier, Amsterdam, 4: 607-629.

Robertson A.H.F., 2002. Overview of the genesis and emplacement of Mesozoic ophiolites in the Eastern Mediterranean Tethyan region. Lithos, 65: 1-67.

Robertson A.H.F. and Dixon J.E., 1984. Introduction: aspects of the geological evolution of the Eastern Mediterranean. In: A.H.F. Robertson and J. Dixon (Eds.), Tectonic evolution of the Eastern Mediterranean. Geol. Soc. London Spec. Publ., 17: 1-74.

Robertson A.H.F., Dixon J.E., Brown S., Collins A., Morris A., Pickett E., Sharp I. and Ustaömer T., 1996. Alternative tectonic models for the Late Palaeozoic-Early Tertiary development of Tethys in the Eastern Mediterranean region, In: A. Morris and D.H. Tarling (Eds.), Paleomagnetism and tectonics of the Mediterranean Region. Geol. Soc. London Spec. Publ., 105: 239-263.

Ricou L.-E., Burg J.-P., Godfriaux I. and Ivanov Z., 1998. The Rhodope and Vardar: the metamorphic and the olistostromic paired belts related to the Cretaceous subduction under Europe. Geodin. Acta, 11: 285-309.

Rubatto D., 2002. Zircon trace element geochemistry: partitioning with garnet and the link between U-Pb ages and metamorphism. Chem. Geol., 184: 123-138.

Şengör A.M.C, Yilmaz Y. and Sungurlu O., 1984. Tectonics of the Mediterranean Cimmerides: nature and evolution of the western termination of Palaeo-Tethys. In: A.H.F Robertson and J.E. Dixon (Eds.), Tectonic evolution of the Eastern Mediterranean. Geol. Soc. London Spec. Publ., 17: 77-112.

Sláma J., Košler J., Condon D.J., Crowley J.L., Gerdes A., Hanchar J.M. and Whitehouse M.J., 2008. Plešovice zircon - a new natural reference material for U-Pb and Hf isotopic microanalysis. Chem. Geol., 249: 1-35.

Soldatos T. and Christofides G., 1986. Rb-Sr geochronology and origin of the Elatia Pluton, Central Rhodope, North Greece. Geol. Balc., 16: 15-23.

Stampfli G.M., 2000. Tethyan oceans. In: E. Bozkurt, J.A. Winchester and J.D.A. Piper (Eds.), Tectonics and magmatism in Turkey and surrounding region. Geol. Soc. London Spec. Publ., 173: 1-23.

Stampfli G.M. and Borel G.D., 2002. A plate tectonic model for the Paleozoic and Mesozoic constrained by dynamic plate boundaries and restored synthetic oceanic isochrons. Earth Planet. Sci. Lett., 196: 17-33.

Stampfli G.M. and Kozur H.W. 2006. Europe from the Variscan to the Alpine cycles. In: D.G.W. Gee and R.A. Stephenson (Eds.), European lithosphere dynamics. Geol. Soc. London Mem., 32: 57-82.

Stampfli G.M. and Hochard C., 2009. Plate tectonics of the Alpine realm. In: J.B. Murphy, J.D Keppie. and A.J. Hynes (Eds.), Ancient orogens and modern analogues. Geol. Soc. London Spec. P ubl., 327: 89-111.

Stampfli G.M., Hochard C., Verard C., Wilhelm C. and von Raumer J., 2013. The formation of Pangea. Tectonophysics, 593: 1-19.

Storck J.-C., Wotzlaw J.-F., Karakas Ö., Brack P., Gerdes A. and Ulmer P., 2020. Hafnium isotopic record of mantle-crust interaction in an evolving continental magmatic system. Earth Planet. Sci. Lett., 535: 116100.

Sun S.S. and McDonough W.F., 1989. Chemical and isotopic systematics of ocean basalts: implications for mantle composition and processes. In: A.D. Saunders and M.J. Norry (Eds.), Magmatism in ocean basins. Geol. Soc. London Spec. Publ., 42: 313-345.

Tatsumi Y. and Eggins R., 1995. Subduction zone magmatism. Blackwell Science, Cambridge, pp. 211.

Tiepel U., Eichhorn R, Loth G., Rohrmülle J., Höll R. and Kennedy A., 2004. U-Pb SHRIMP and Nd isotopic data from the western Bohemian Massif (Bayerischer Wald, Germany): Implications for Upper Vendian and Lower Ordovician magmatism. Intern. J. Earth Sci., 93: 782-801.

Turpaud P. and Reischmann T., 2010. Characterization of igneous terranes by zircon dating: implications for UHP occurrences and suture identification in the Central Rhodope, northern Greece. Intern. J. Earth Sci., 99: 567-591.

Vermeesch P., 2018. IsoplotR: a free and open toolbox for geochronology. Geosci. Front., 9: 1479-1493, doi: 10.1016/j.gsf.2018.04.001.

von Quadt A. and Peytcheva I., 2005. The southern extension of Srednogorie type Upper Cretaceous magmatism in Rila-western Rhodopes: constraints from isotope-geochronological and geochemical data. Proc. Ann. Int. Conf. 80th Anniv. Bulg. Geol. Soc., p. 113-116.

Whitney D.L. and Evans B.W., 2010. Abbreviations for names of rock-forming minerals. Am. Miner., 95: 185-187.

Wiedenbeck M., Alle P., Corfu F., Griffin W., Meier M., Oberli F., Quadt A.V., Roddick J. and Spiegel W., 1995. Three natural zircon standards for U-Th-Pb, Lu-Hf, trace element and REE analyses: Geostand. Newslett., 19: 1-23.

Zagorchev I.S., 1998. Pre-Priabonian Paleogene formations in southwest Bulgaria and northern Greece: stratigraphy and tectonic implications. Geol. Mag., 135: 101-119.

Zagorchev I.S., Moorbath S. and Lilov P., 1987. Radiogeochronological data on the Alpine igneous activity in the western part of the Rhodope Massif. Geol. Balc., 17: 59-71.